Coupling models of within-human, human-to-mosquito, and within-mosquito parasite dynamics to identify key drivers of malaria transmission

Xiao Sun[1], Matthew W. A. Dixon[2,3], James S. McCarthy[2,3,4], James M. McCaw[1,5,*], Pengxing Cao[1,*]

[1] School of Mathematics and Statistics, The University of Melbourne, Melbourne, VIC, Australia

[2] Department of Infectious Diseases, The Peter Doherty Institute, The University of Melbourne, Parkville, VIC, Australia

[3] Walter and Eliza Hall Institute, Parkville, VIC, Australia

[4] Victorian Infectious Diseases Service, The Royal Melbourne Hospital, Parkville, Victoria, Australia

[5] Melbourne School of Population and Global Health, The University of Melbourne, Melbourne, VIC, Australia

[*] Correspondence: jamesm@unimelb.edu.au; pengxing.cao@unimelb.edu.au

Abstract

The transmission of malaria parasites from humans to mosquitoes is an essential element of the parasite life cycle. However, human-to-mosquito transmission remains poorly characterized due to insufficient quantification of biological parameters and limited tools for systematic study. To fill this knowledge gap, a mathematical modeling approach using data from a malaria human challenge study was used to estimate the ratio of the number of viable male gametes produced within a mosquito to the number of male gametocytes taken in a blood meal (0.80, 95% highest density posterior interval (HDPI): 0.13–2.90), and the probability of fertilization for per pair of viable male and female gametes (0.029, 95% HDPI: 0.006–0.109). Drawing on these quanti-

tative results, we developed a multi-scale model of human-to-mosquito transmission to identify the dominant host factors determining a human's infectiousness to mosquitoes. Our primary findings are that, for individuals with asymptomatic infections, 1) the time from exposure to the onset of infectiousness is primarily driven by parameters governing asexual parasite multiplication and in-human gametocyte maturation; and 2) for those with established infection, infectiousness is predominantly influenced by the availability of gametocytes in the circulating blood for uptake in a blood meal and the gamete fertilization efficiency.

Introduction

Malaria infection is a vector-borne disease that continues to pose a health threat to billions of people worldwide, causing approximately 610,000 deaths in 2024 [1]. The transmission of malaria parasites from the human host to a female Anopheles mosquito occurs when the mosquito feeds on the blood of the infected individual and ingest at least one male and one female mature gametocyte [2]. Those gametocytes undergo rapid transition into gametes, with each male gametocyte producing eight microgametes. Male microgametes and female macrogametes then undergo meiosis in the mosquito midgut to form diploid ookinetes that invade the midgut wall and divide to form oocysts. Each oocyst matures to release thousands of haploid sporozoites which move to the salivary gland of the mosquito, ready for transmission back to a human to cause a new infection, thus sustaining the population of parasites in the ecosystem. This process can be investigated experimentally by performing either direct feeding assay (DFA) on infected individuals, or by standard membrane feeding assays (SMFA) where infected blood is placed in a special feeding container for mosquitoes to feed on. Mosquitoes can be examined for the presence of oocysts or sporozoites; the proportion of mosquitoes developing oocysts or sporozoites provides a direct measurement of the probability that a mosquito will become infected or infectious after taking a blood meal from the infected human (referred to as the human-to-mosquito transmission probability). Such assays are widely used to experimentally evaluate both the infectiousness of infected human hosts to mosquitoes and the efficacy of interventions, such as drugs or vaccines to block transmission [3–5].

For falciparum malaria, quantitative understanding of the process of parasite transmission from a human to a mosquito remains incomplete, despite the availability of substantial mosquito feeding assay data collected over many years. This gap can be attributed to two main factors.

The first is the incomplete quantification of key biological parameters that influence human-to-mosquito transmission. In particular, two biological parameters that drive gamete development and fertilization have not yet been rigorously estimated. One is the ratio of viable male gametes produced within a mosquito to male gametocytes taken in a blood meal (hereafter referred to as the male gamete-to-gametocyte ratio). Theoretically, this ratio has an upper bound of eight, as each male gametocyte produces up to eight male gametes [6]. However, the true value is expected to be substantially lower, since not all male gametes remain viable during replication and differentiation and therefore are incapable of successful fertilization [7–9]. The other parameter is the probability of successful fertilization between a viable male and female gamete. The absence of estimates for this parameter in the literature likely reflects several limitations, including the lack of experimental studies quantifying all key parasite populations (e.g., male and female gametes and zygotes/oocysts), as well as the scarcity of modeling studies specifically designed to quantify the fertilization process.

The second factor contributing to our incomplete understanding of human-to-mosquito transmission is the lack of tools designed to quantitatively assess the effects of various host (human and mosquito) factors on the human-to-mosquito transmission probability. A direct approach to overcome this limitation would be to conduct deliberate clinical, experimental or observational studies to collect such data. Previous studies have focused predominantly on how the level of gametocytemia in human hosts influences the transmission probability. As illustrated in Fig. 1, where mosquito feeding assay data from three representative experimental studies are presented [10–12], there remains substantial unexplained variability in both gametocytemia and transmission probability when other host factors are not considered. The variability is particularly evident in asymptomatic infections, where transmission outcomes are highly heterogeneous across individuals and not solely determined by gametocyte density [13]. Notably, human-to-mosquito transmission can occur even at a low gametocyte density, indicating that asymptomatic infections may contribute to onward transmission and therefore comprise an important part of the human infectious reservoir [14]. This has significant public health implications for implementing strategies to interrupt malaria transmission and highlights the importance of understanding the main drivers of human-to-mosquito transmission. Experimental investigations to fill these gaps would require substantial resources. An alternative approach is to conduct *in silico* experiments using mathematical models calibrated to available data. However, this approach requires models that not only capture both established and hypothesized mechanisms

underlying key biological processes in human-to-mosquito transmission, such as gametocyte development in humans, parasite uptake during mosquito feeding, and parasite development within mosquitoes, but models that are also parameterized in a way that allows estimation of those parameters from available data. Although numerous models have been developed to study within-host malaria dynamics and transmission, there exists an important gap with a lack of a comprehensive model of human-to-mosquito transmission. Existing models that examine aspects of human-to-mosquito transmission either lack within-mosquito dynamics [15–20], omit blood-stage dynamics [21–25], or incorporate overly simplified components [26, 27].

Here, we develop and combine two mathematical models to estimate key biological parameters and investigate the relative importance of various host factors—including those governing gametocyte development in humans and those driving sporozoite development in mosquitoes—that determine the probability of human-to-mosquito transmission. The first model captures both gametocyte uptake by mosquitoes and parasite development within mosquitoes to describe mosquito feeding (hereafter referred to as the mosquito feeding model). The mosquito feeding model was fitted to direct feeding assay data from a volunteer infection study (VIS; i.e., Collins et al. data reproduced in Fig. 1) to estimate the two biological parameters, which have not, to date, been well quantified. The second model integrates the mosquito feeding model with an existing data-calibrated within-human parasite dynamics model [19, 20] (hereafter referred to as the human-to-mosquito transmission model); this model incorporates key host factors governing the full process of human-to-mosquito transmission, from asexual blood-stage expansion in humans to sporozoite formation in mosquitoes. The human-to-mosquito transmission model was used to characterize the probability of human-to-mosquito transmission in asymptomatic infections, and identify the key factors that influence this probability through sensitivity analysis.

Results

Estimation of key biological parameters driving gamete development and fertilization

The male gamete-to-gametocyte ratio (ρ) and the probability of successful fertilization between a viable male gamete and a viable female gamete (p_f) are key biological parameters influencing human-to-mosquito transmission of the malaria parasite, yet are poorly characterized in the

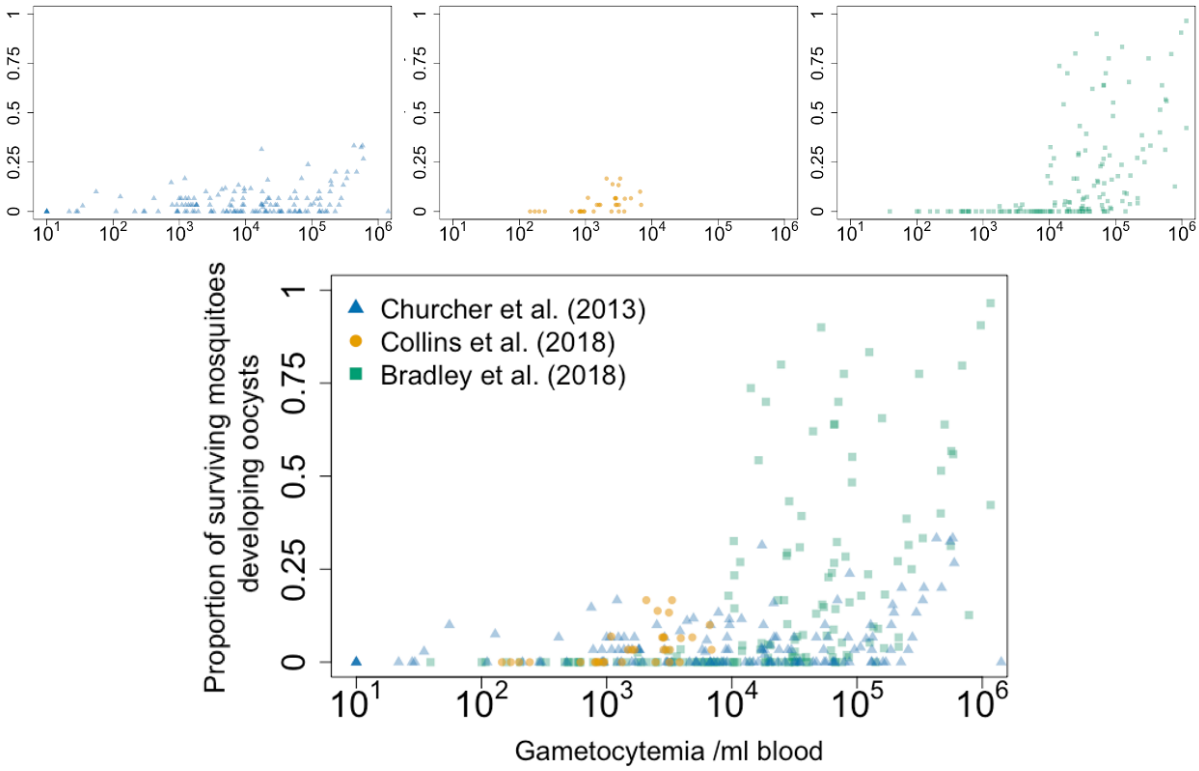

Figure 1: **Direct feeding assay data from three representative experimental studies.** Each data point represents a sample of gametocytemia collected from an infected human and the proportion of surviving mosquitoes that developed oocysts following a blood meal from the infected human and subsequently developed oocysts. Blue triangles represent data from Churcher et al. [10]. Yellow dots represent data from Collins et al. [11]. Green squares represent data from Bradley et al. [12].

literature. To estimate these parameters, the mosquito feeding model was fitted to a set of direct feeding assay data from a previously published VIS study by Collins et al. [11]. The VIS data used in model fitting includes the longitudinal measurements of female and male gametocytemia from 11 volunteers and the proportion of mosquitoes developing oocysts associated with each pair of gametocytemia measurements for each volunteer. The mosquito feeding model is a set of mathematical equations and statistical distributions that parameterize the turnover dynamics of parasites of different developmental stages from gametocytes to oocysts and sporozoites. Model fitting was conducted using an approximate Bayesian computation (ABC) algorithm to sample the parameter values with which the solutions to the mosquito feeding model match the longitudinal measurements based on a metric for goodness of fit. Details on the data, the model, the fitting algorithm, and statistical diagnostics are provided in the Materials and Methods.

The model fitting results are shown in Fig. 2. Panels A and B show model posterior esti-

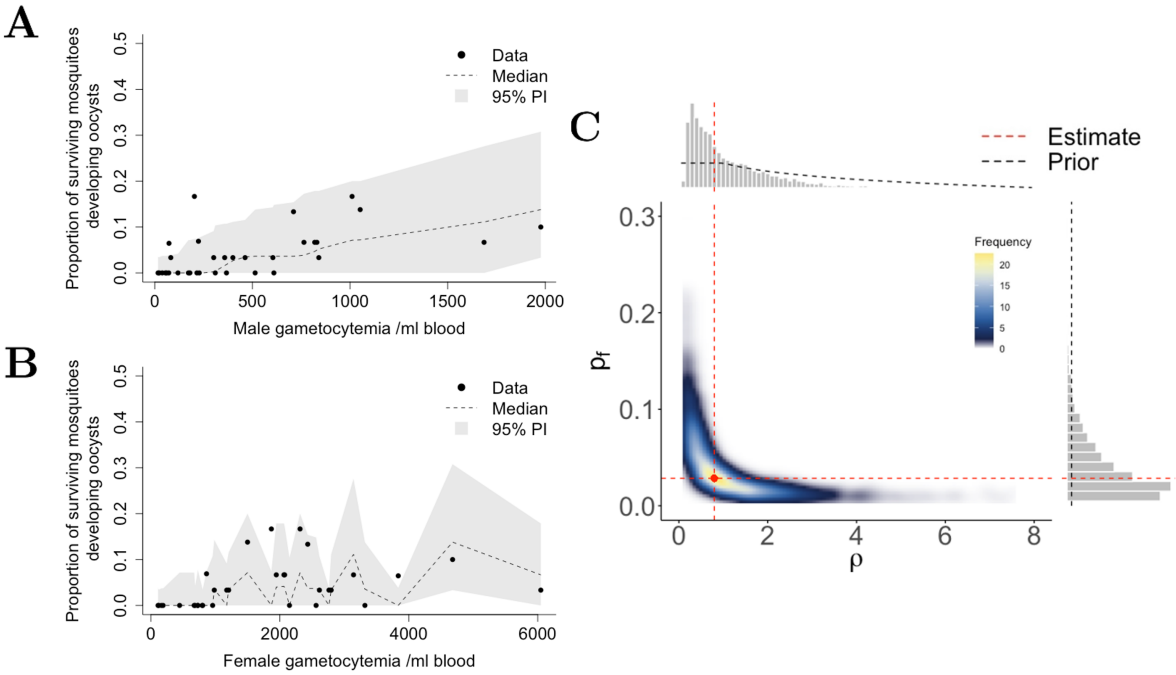

Figure 2: **Results of model fitting and parameter estimation.** (A) and (B) show model posterior estimates with experimental observations. The black dashed line shows the median prediction obtained from the model fitting process, and the grey shaded area shows the 95% prediction interval (PI). Data are presented by black dots. (C) shows the joint and marginal distributions of 5,000 draws from the posterior (i.e., estimate) for the male gamete-to-gametocyte ratio (ρ) and the probability of successful fertilization per gamete pair (p_f). Black dashed curves indicate the prior distributions of the parameters. The red lines intersect at the MAP estimates (the point with the highest posterior density).

mates with experimental observations, and panel C shows the distribution of parameter values sampled by the ABC algorithm (i.e., the posterior distribution). Detailed male and female gametocytemia data for each volunteer at each feeding time point are shown in S1 Fig. The corresponding data on the proportion of mosquitoes developing oocysts at each time point, with the model fitting results, are shown in S2 Fig. The trends of the data are well captured by the median model predictions; likewise the variance in the data can be explained by the 95% prediction intervals (PI). The posterior distribution provides the maximum a posteriori (MAP) estimate, which is the combination of parameters (ρ and p_f) that is most well supported (i.e., has the highest density in the posterior distribution), and the estimated 95% highest density posterior interval (95% HDPI, which contains approximately 95% of the samples in the posterior distribution) for the two biological parameters ρ and p_f. For the male gamete-to-gametocyte ratio ρ, the MAP estimate is 0.80 (with a 95% HDPI of 0.13–2.90), suggesting that every ten male gametocytes taken by a mosquito blood meal lead to the formation of on average eight viable male gametes available for fertilization in the mosquito midgut (implying an attrition

rate of 90% from the theoretical maximum of eight male microgametes arising from one male gametocyte). The MAP estimate for the probability of gamete fertilization per gamete pair p_f is 0.029 (95% HDPI: 0.006–0.109). The large variance in parameter estimates (indicated by the 95% HDPI) reflects limited information content in the experimental data, whereby substantially different parameter combinations—high ρ with low p_f or conversely low ρ with high p_f—produce comparable measures of goodness of fit. This relationship is clearly reflected in the hyperbolic structure of the posterior distribution shown in Fig. 2C).

Characterizing malaria transmission from an asymptomatic infected individual to mosquitoes

Symptomatic *P. falciparum* is not universal, with many people in endemic areas carrying parasites in their blood without symptoms, a situation referred to as clinical immunity [28, 29]. As they frequently carry circulating gametocytes, they can serve as reservoirs for onward transmission to mosquitoes [13, 30] Historically, characterizing the infectiousness of asymptomatic individuals to mosquitoes has relied on mosquito feeding assays, which are costly and logistically complex, making them impractical for assessing the relative importance of host factors in determining the probability of human-to-mosquito transmission. Here, we address this gap by coupling the mosquito feeding model calibrated to the VIS data (presented above) with a previously developed within-human parasite dynamics model that describes the temporal dynamics of asexual parasitemia and gametocytemia following blood-stage infection [19, 20] (see the Materials and Methods for details). The coupled model (referred to as the human-to-mosquito transmission model) provides a platform for linking human and mosquito factors (within-host level) with transmission probability (epidemiological level).

Fig. 3A illustrates two simulated time series of asexual parasitemia generated using the human-to-mosquito transmission model: one with parasitemia fluctuating around approximately 10^4 parasites/mL blood—a level commonly observed in asymptomatic infections in low transmission settings [5, 31, 32], and the other with parasitemia fluctuating around approximately 10^6 parasites/mL—a level typically observed in asymptomatic infections in high transmission settings [5, 13, 28, 32]. Details of the simulation procedure are provided in Materials and Methods. Note that the simulated time series of asexual parasitemia includes an initial exponential growth phase, consistent with observations from VIS trials [11], although this phase is rarely captured

in field studies due to its short duration relative to typical sampling frequency, followed by a transition to a dynamic regime, across which asexual parasitemia fluctuates around a relatively stable level, as observed in longitudinal cohort studies [33, 34]. Fig. 3B shows, for the two simulated infections from Fig. 3A, how the human-to-mosquito transmission probability changes over time following a bite. This probability is defined as the probability that a mosquito taking a blood meal at a particular time (in days, post infection of the human) develops oocysts (see the Materials and Methods for details). The transmission probability (per bite) curve for the simulated high asexual parasitemia individual is much higher than for the simulated low asexual parasitemia individual.

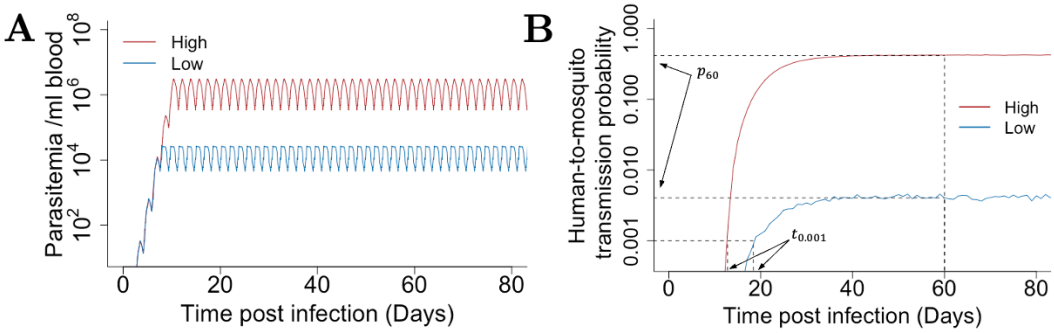

Figure 3: **Human-to-mosquito transmission probability of asymptomatic infections.** (A) Simulated trajectories of asexual parasitemia in asymptomatic infections fluctuate around immune-regulated set-point densities of 10^4 (low transmission settings, blue) and 10^6 (high transmission settings, red). (B) The human-to-mosquito transmission probabilities associated with the parasitemia trajectories in (A). For each time point, we simulated the mosquito feeding model with 100,000 mosquitoes, and the transmission probability is given by the proportion of surviving mosquitoes developing oocysts (details for the simulations are provided in the section of Simulation of mosquito feeding assays and calculation of the human-to-mosquito transmission probability in the Materials and Methods). The choice of 100,000 mosquitoes, which is substantially larger than that used in empirical mosquito feeding experiments, provides a more accurate prediction of the transmission probability to support subsequent sensitivity analysis.

The period following infection until any parasites appear in the blood is referred to as the prepatent period, while the onset of infectiousness (of the human to a mosquito) does not occur until mature gametocytes have developed (typically approximately 14 days for *P. falciparum*). While in simple models of contagiousness such as the Ross–MacDonald model, a delay between infection and infectiousness (known as the latent period) can be incorporated, the level of infectiousness is fixed throughout the infectious period [35]. In reality, and our model (Fig. 3B), the number of gametocytes circulating increases as more are produced with rising parasitemia, until a stable level is reached. Therefore the probability (per bite) of infection increases (and

may later stabilize) rather than undergoing a discrete switch in which a human changes from being non-infectious to infectious. Two quantities were defined to enable us to assess which biological parameters most strongly influence the transmission probability in the increasing and stable phases:

- The time at which the transmission probability first surpasses a specific threshold (denoted by $t_{0.001}$), which characterizes the critical early (increasing) phase of the human to mosquito infection process. Specifically, we define $t_{0.001}$ as the time post-infection at which the probability of a mosquito becoming infected from a single blood meal reaches 0.001 (i.e., 1 in 1,000 chance of a mosquito becoming infected given a blood meal) (Fig. 3B). Using an alternative threshold (i.e., $t_{0.0005}$) does not affect the results of the subsequent analysis, as will be demonstrated in the following sections whenever relevant.

- The human-to-mosquito transmission probability at day 60 post-infection (denoted by p_{60}), chosen as a representative time point given the prolonged duration of asymptomatic infections [30]. This quantity serves as a surrogate for the steady-state transmission probability.

These two metrics ($t_{0.001}$ and p_{60}) effectively capture, and so summarize, how the transmission probability (and its dependence on time-since-exposure) differs between the two malaria transmission settings. They are therefore suitable metrics for use in subsequent sensitivity analyses.

Determinants of human-to-mosquito transmission probability in asymptomatic infections

To investigate the relative importance of different host factors in determining the probability of human-to-mosquito transmission, a global sensitivity analysis was conducted using the Latin Hypercube Sampling-Partial rank correlation coefficient (LHS-PRCC) method (see Materials and Methods) [36]. The sensitivity analysis quantifies how different host factors (i.e., model parameters that capture the associated biological processes) influence the human-to-mosquito transmission probability in asymptomatic infections (characterized by $t_{0.001}$ and p_{60}). We first examine the high-transmission setting, as it is the context in which asymptomatic infections are more frequently observed [37, 38].

For $t_{0.001}$, sensitivity analysis (Fig. 4A) shows that it is predominantly influenced by three bi-

ological factors: the parasite death rate (δ_p), the replication number of asexual parasites (r_p), and the maturation rate of gametocytes (m). Note that PRCC values closer to 1 or -1 indicate a stronger positive or negative correlation, respectively, whereas values closer to 0 indicate a weaker correlation. The result remains valid for other choices of the threshold used to define $t_{0.001}$; for example, changing $t_{0.001}$ to $t_{0.0005}$ in the PRCC analysis does not alter the findings (see S3 Fig). The death rate of parasites δ_p and the parasite replication number r_p are the key parameters determining the multiplication number of parasites per asexual replication cycle, commonly referred to as the parasite multiplication rate (PMR). Since PMR can vary significantly across individuals due to biological heterogeneity within human hosts [39], substantial variation in $t_{0.001}$ is expected, even though this is challenging to observe in field studies. The marginal relationships across the LHS-sampled parameter space between δ_p, r_p and m (the three dominant factors identified by the PRCC analysis) and $t_{0.001}$ are presented in Fig. 4B. These marginal relationships show that a higher value of δ_p is associated with a longer $t_{0.001}$ (as indicated by the median curve) whereas higher values of r_p and m are associated with a shorter $t_{0.001}$. Marginal relationships for all parameters are presented in S4 Fig. Mosquito-related factors are generally less influential in determining $t_{0.001}$, including the two parameters we estimated earlier: the male gamete-to-gametocyte ratio ρ and the probability of gamete fertilization p_f.

The PRCC analysis of the steady-state transmission probability (approximated by p_{60}) shows that p_{60} is predominantly determined by six factors, including three human-related parameters: the sexual conversion rate (f), the fraction of male gametocytes (f_g), and the death rate of circulating gametocytes (δ_{gc}), as well as all three mosquito parameters: the blood meal volume (V), the male gamete-to-gametocyte ratio (ρ), and the probability of fertilization (p_f) (Fig. 5). The marginal relationships between f, f_g, δ_{gc}, V, ρ and p_f (the six dominant factors identified by the PRCC analysis) and p_{60} are presented in Fig. 5B to illustrate the dependency and uncertainty, with results for all parameters examined in the PRCC analysis provided in S5 Fig. Notably, all of these parameters are distinct from those that were dominant in the analysis of $t_{0.001}$ (i.e., δ_p, r_p and m), indicating that the period $t_{0.001}$ and the steady-state transmission probability are governed by distinct biological mechanisms.

Finally, a similar set of PRCC analyses were performed to examine the relative importance of different host factors in determining the human-to-mosquito transmission probability in the low

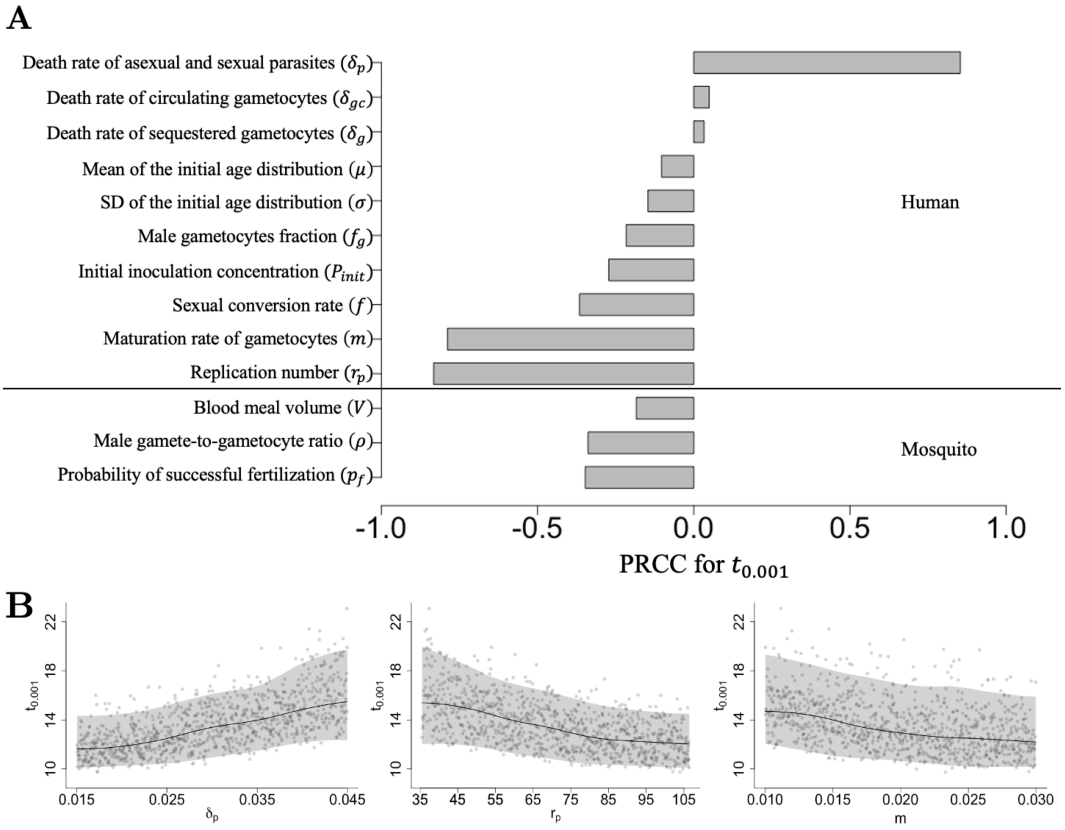

Figure 4: **Sensitivity analysis of parameters for $t_{0.001}$.** (A) shows the PRCC results of a set of model parameters with respect to $t_{0.001}$. The parameters include those representing host factors in humans as well as those associated with mosquitoes. PRCC values closer to 1 or -1 indicate a stronger positive or negative correlation, respectively, whereas values closer to 0 indicate a weaker correlation. (B) illustrates the marginal relationships between $t_{0.001}$ and the three parameters with the highest absolute PRCC values, which are the parasite death rate δ_p, the replication number of asexual parasites r_p, and the maturation rate of gametocytes m, based on the LHS-sampled parameter space. Predicted $t_{0.001}$ for individual LHS-sampled parameter values are presented by black dots. The median predictions are represented by solid curves, and the 95% PIs are represented by shaded areas.

transmission setting (as per Fig. 3A). For both $t_{0.001}$ and p_{60}, the leading host factors identified in the analysis for the high transmission setting are the same in low transmission setting. However, some notable quantitative differences are observed compared to the high transmission setting for $t_{0.001}$. The gametocyte maturation rate (m) becomes the most influential parameter for $t_{0.001}$ in low transmission setting, while it ranked third in the analysis of the high transmission setting (see S6 Fig). Although the gametocyte maturation rate is governed by intrinsic regulatory programs and is not directly amenable to intervention [40], this result highlights the importance of gametocyte development dynamics in shaping transmission. The parasite death rate (δ_p) and the parasite replication number (r_p) move to a lower position in the ranking. These changes reflect a reduced impact of δ_p and r_p when the parasitemia levels in asymptomatic infections

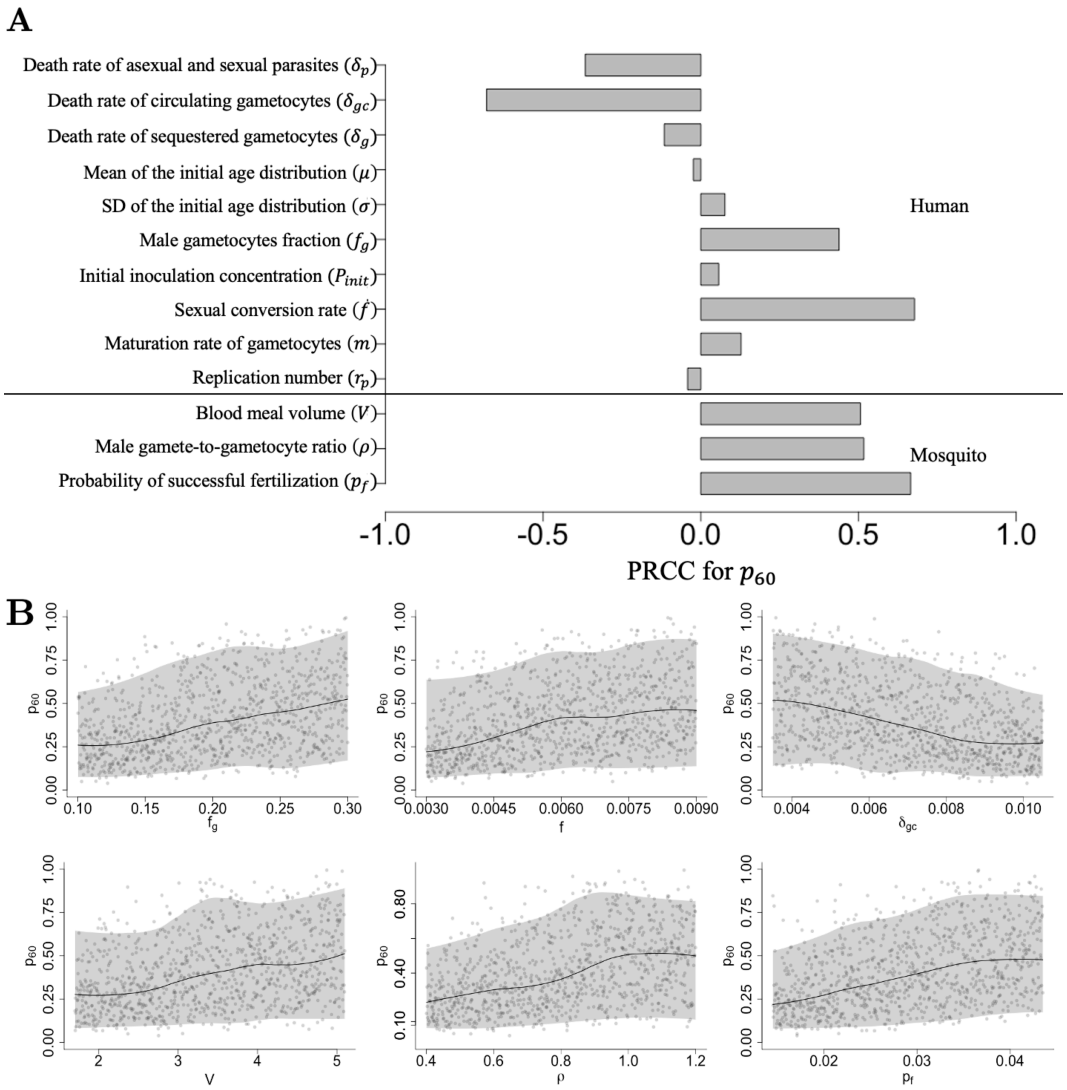

Figure 5: **PRCC results and sensitivity of parameters for the steady-state infectiousness p_{60}.** (A) shows the PRCC results of a set of model parameters with respect to p_{60}. The parameters include those representing host factors in humans as well as those associated with mosquitoes, and they are presented in the same order as in Fig. 4. PRCC values closer to 1 or -1 indicate a stronger positive or negative correlation, respectively, whereas values closer to 0 indicate a weaker correlation. (B) illustrates the marginal relationships between p_{60} and the six parameters with the highest absolute PRCC values, which are the sexual conversion rate f, the fraction of male gametocytes f_g, and the death rate of circulating gametocytes δ_{gc}, the blood meal volume V, the male gamete-to-gametocyte ratio ρ, and the probability of fertilization p_f, based on the LHS-sampled parameter space. Predicted p_{60} for individual LHS-sampled parameter values are presented by black dots. The median predictions are represented by solid curves, and the 95% PIs are represented by shaded areas.

are lower. For p_{60}, the six predominant host factors are likewise maintained as those identified in high transmission setting (see S7 Fig).

Discussion

In this study, we have developed a multi-scale model of human-to-mosquito malaria transmission that combines parasite dynamics in both humans and mosquitoes. Through application to experimental data, we have used the model to estimate several biological parameters, thereby quantifying the effects of various human and mosquito factors on the human-to-mosquito transmission probability. Our primary findings include: (1) the estimation of two key biological parameters, the male gamete-to-gametocyte ratio ρ, and the probability of successful fertilization of a female by a male gamete p_f; (2) the characterization of the probability of parasite transmission from asymptomatic infected individuals to mosquitoes; and (3) the identification of the relative importance of different host factors in determining the human-to-mosquito transmission probability. Our study improves the quantitative understanding of the biological determinants of malaria parasite transmission from human hosts to mosquitoes and provides a data-analytic framework that integrates mathematical models, human challenge data and statistical inference to study malaria infection and transmission.

The male gamete-to-gametocyte ratio ρ was estimated to be 0.80 (95% HDPI: 0.13–2.90), which can be used to further quantify the underlying processes that determine this parameter. Specifically, ρ is defined as the product of two biological parameters: the fraction of male gametocytes that are able to produce male gametes via replication (denoted by p_g) and the number of fertile male gametes that are produced by each male gametocyte (denoted by α), i.e., $\rho = p_g\alpha$. If α is assumed to be three—based on previous findings that each male gametocyte undergoing meiosis can produce eight gametes [6] with approximately 40% or fewer of the gametes viable for fertilization [7]—we obtain a rough estimate for p_g of 0.27 (uncertainty: 0.043–0.97). This emphasizes the high uncertainty in the fraction of male gametocytes that are capable of differentiating into fertile gametes.

Our estimate for the probability of successful fertilization p_f between a viable macrogamete and a viable microgamete of 0.029 (95% HDPI: 0.006–0.109) suggests that only a small proportion of viable gamete pairs undergo successful fertilization. In our model, p_f is defined as the probability of successful fertilization per pair of viable male and female gametes and may be interpreted as arising from either (or both) the chance that a male gamete encounters a female gamete, and that, upon encounter, fertilization occurs. While previous modeling studies have examined within-mosquito dynamics [21–23], the process of fertilization in these models is typically

represented as a rate parameter (i.e., per viable gamete pair per day), with parameter values chosen to yield oocyst counts within biologically plausible ranges. To the best of our knowledge, no experimental or modeling studies have provided an *in vivo* estimate of the probability of successful fertilization for each pair of viable female and male gametes. Our study therefore advances the quantitative understanding of the fertilization process. However, the available data are insufficient to unambiguously identify ρ and p_f, as evidenced by the correlation in the posterior distribution shown in Fig. 2. Future mosquito feeding experiments, particularly those in which time series data on the numbers of female and male gametocytes and oocysts in mosquitoes are collected, may help resolve this parameter non-identifiability issue.

Previous longitudinal observations show that parasitemia in asymptomatic infections fluctuates around a relatively stable level over time [33, 34]—a pattern that can be interpreted in light of hypothesized host immune responses that act to reduce parasite multiplication rates [30, 41]. We simulated time series of asexual parasitemia consistent with this behavior following an initial growth phase (Fig. 3A). Another dataset, from malaria-naïve neurosyphilis patients undergoing malaria therapy, exhibits a markedly different pattern of parasitemia [42, 43]. In contrast to the stabilized parasitemia commonly observed in field studies, these neurosyphilis patients, although asymptomatic, displayed multiple irregular spikes in parasitemia, with the first peak reaching approximately 10^8 parasites/mL (a clinically relevant level), followed by progressively lower peaks in subsequent spikes. This parasitemia pattern has been hypothesized to result from the interaction between antigenic variant switching and the gradual development of variant-specific immunity [43]; as variant-specific immune responses develop, parasites preferentially switch to variants for which no specific immunity has been established. While the data from neurosyphilis patients highlight the complex interplay between host immunity and parasite biology in shaping parasitemia trajectories, they may not be a valid representation of the pattern of parasitemia observed in repeatedly exposed, clinically immune asymptomatic individuals in endemic areas. Modeling neurosyphilis patient data, and characterizing the (hypothetical) probability of human-to-mosquito transmission from such individuals, would require additional analyses including different parameter choices and modeling assumptions, and is therefore not within the scope of this work. In addition, the parameter values used to simulate asymptomatic infections were estimated from a single VIS study, in which participants were malaria-naïve, and therefore may not fully reflect the characteristics of asymptomatic infections in endemic settings. Incorporating additional data from endemic settings is therefore a future priority to

improve the biological relevance of our work.

The sexual conversion rate f is an important parameter driving the kinetics of gametocytemia, which mediates transmission from humans to mosquitoes. Our analyses show that although f is less influential in determining $t_{0.001}$ in asymptomatic infections, it can strongly influence the steady-state human-to-mosquito transmission probability p_{60}, which represents longer-term behavior and therefore is expected to have a much stronger impact in shaping the transmission pattern compared to $t_{0.001}$. This suggests that a refined model of the sexual conversion process, particularly one incorporating the effects of parasite genetics, immunity and antimalarials [44–46], might be useful in further elucidating the determinants of transmission probability that are not captured in our current model. For example, some evidence suggests that genetic polymorphisms associated with the development of artemisinin resistance may increase the sexual conversion rate and thus result in increased transmission efficiency. Furthermore, longitudinal observations suggest that the ratio of parasitemia to gametocytemia can vary over time within a single infected individual [47], which may reflect temporal variation in the sexual conversion rate. Accounting for this temporal variation may improve model realism and should be explored in future work.

Due to the emergence and geographical spread of antimalarial resistance, there is growing interest in deploying transmission-blocking interventions, such as gametocytocidal drugs or transmission blocking vaccines, to accelerate malaria elimination [48]. For example, primaquine is highly effective against mature gametocytes, and has therefore been advocated as an addition to standard artemisinin combination therapy for its transmission-blocking effect [49]. In addition, considerable effort is being devoted to the development of transmission blocking vaccines aimed at reducing the probability of successful human-to-mosquito transmission [50]. Our human-to-mosquito model, which maps human parasite dynamics to human infectiousness to mosquitoes, can be incorporated into a multi-scale epidemiological model of malaria transmission to predict the clinical and public health impact of these transmission-blocking strategies, providing valuable insights for optimizing and implementing effective malaria control strategies.

Materials and Methods

Methods for model fitting

This section includes: (1) mosquito feeding assay data used in model fitting; (2) a stochastic model of mosquito feeding, which captures the transmission of gametocytes from humans to mosquitoes and their subsequent development within the mosquito; and (3) methods of model fitting to estimate biological parameters.

Data

The data used in the modeling study are from a previously published VIS [11], in which 17 healthy adult volunteers were inoculated with *P. falciparum*–infected red blood cells. The VIS was approved by the QIMR Berghofer Human Research Ethics Committee and registered with ClinicalTrials.gov (NCT02431637 and NCT02431650). Following inoculation, participants were monitored longitudinally, with quantitative PCR used to measure gametocytemia throughout the experiment. Mosquito feeding assays were performed for 11 of the 17 participants to assess the transmission of gametocytes from humans to mosquitoes. The data used in model fitting includes male and female gametocyte densities measured by PfMGET and Pfs25 qRT-PCR respectively and the proportion of mosquitoes developing oocysts detected by an 18S rDNA qPCR assay.

Mosquito feeding model

A mathematical model was developed to describe the mosquito feeding experiments (referred to as the mosquito feeding model). The mosquito feeding model extends the within-mosquito model developed in [25] to include a probabilistic component to capture the process of gametocyte transmission from human to mosquito. The mosquito feeding model captures the stages of the lifecycle within the mosquito from gametocytes into oocysts and sporozoites, each of which are important developmental stages of the malaria parasite in the mosquito. Following [25], transition times from a pre-oocyst parasite stage (which is explicitly modeled as zygotes in our model) to oocysts and from oocysts to sporozoites are modeled, and the model does not include any outflow due to the death of parasites within the mosquito during the development process from zygotes to sporozoites. The oocyst or sporozoite are the target development stage for measurement in mosquito feeding assays [51–53]. Since the human-to-mosquito transmission

probability depends only on the presence of oocysts or sporozoites, rather than their abundance, the model tracks only the transition times from the establishment of viable oocysts to the onset of sporozoite production, without explicitly modeling sporozoite release from oocysts. Fig. 6 presents a schematic diagram of the model, describing the uptake of gametocytes by a mosquito and their development into sporozoites.

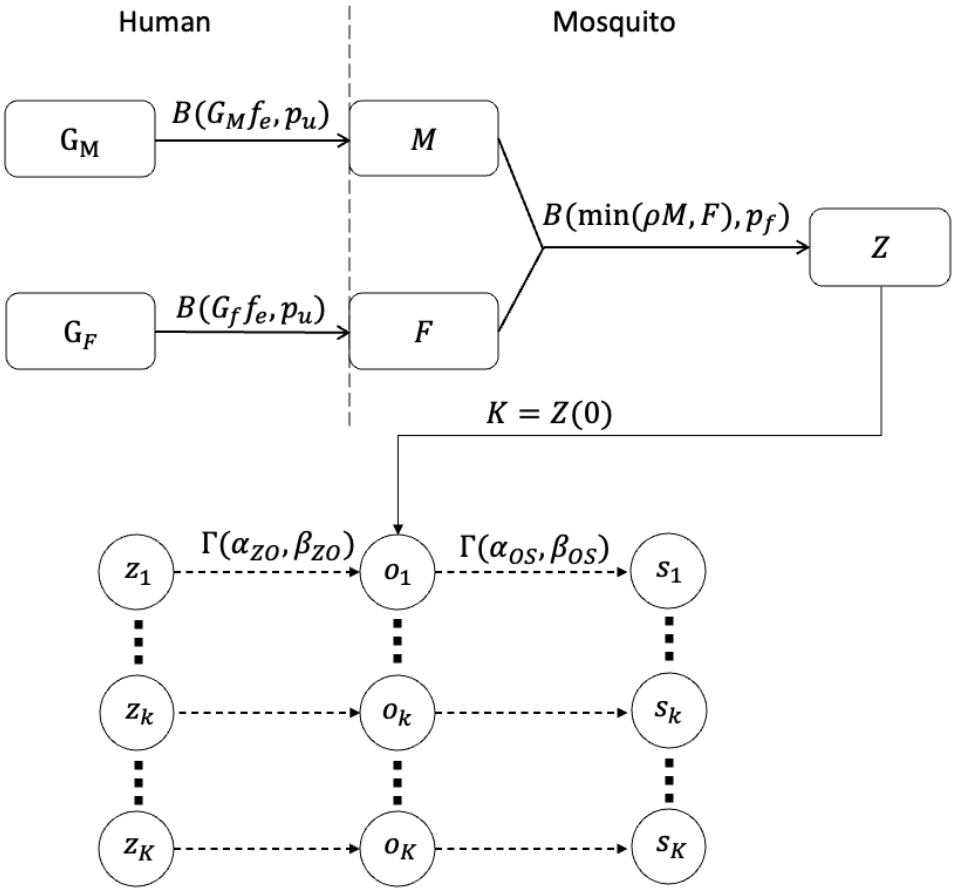

Figure 6: **Mosquito feeding model.** M and F represent the number of male and female gametocytes taken by a single mosquito during a blood meal, sampled from a binomial distribution $\text{Bin}(G_{\{M,F\}} f_e, p_u)$, where G_M and G_F are the number of male and female gametocytes in the bitten human, f_e is the fraction of the total human blood volume V_H localized to the site of a mosquito bite (V_H is assumed to be 4000mL), and p_u is the probability of uptake by the mosquito, which is the ratio of a mosquito blood meal volume V to the volume of blood $f_e V_H$. Z represents the number of zygotes. The initial number of zygotes $Z(\tau = 0)$ is sampled from a binomial distribution $\text{Bin}(\min(\rho M, F), p_f)$, where ρ is the male gamete-to-gametocyte ratio, defined as the product of the fraction of male gametocytes that are able to produce male gametes via meiosis p_g and the number of male gametes that are produced by male gametocytes and viable for fertilization α, and p_f is the probability of successful fertilization for each pair of gametes. Each zygote z_k ($k \in \{1, 2, \ldots, K\}$, $K = Z(0)$) develops into an oocyst o_k with a transition time sampled from a gamma distribution $\Gamma(\alpha_{ZO}, \beta_{ZO})$. Each oocyst o_k then undergoes sporogony and starts producing sporozoites (a state modeled by s_k) after an additional time sampled from a gamma distribution $\Gamma(\alpha_{OS}, \beta_{OS})$.

The number of male gametocytes taken by a mosquito during a blood meal, M, is assumed to follow the binomial distribution:

$$M \sim \mathrm{Bin}(G_M f_e, p_u), \tag{1}$$

where G_M is the total number of male gametocytes in human body and f_e is the fraction of the total human blood volume V_H localized to the site of a mosquito bite. The total number of male gametocytes available for mosquito uptake in a blood meal is given by $G_M f_e$, based on the assumption that circulating male gametocytes are homogeneously distributed throughout the blood. The probability of gametocyte uptake by the mosquito, p_u, is given by $p_u = V/(f_e V_H)$, which is the ratio of a mosquito blood meal volume V to the volume of blood $f_e V_H$ that contains $G_M f_e$ male gametocytes (e.g., assuming a human blood volume of $V_H = 4000$mL, a value of $f_e = 1/4000$ implies that $f_e V_H = 1$mL of blood is localized at the site of mosquito bite, and therefore the maximum number of male gametocyte that can be taken by mosquitoes corresponds to the number of male gametocyte in 1mL of blood). Note that f_e has an upper bound of 1 based on its definition and a lower bound of V/V_H below which the selection probability p_u becomes 1 and the binomial distribution model is no longer valid to capture the biological process. Given the total number of female gametocytes in human body G_F, the number of female gametocytes taken by a mosquito during a blood meal F is similarly defined as follows:

$$F \sim \mathrm{Bin}(G_F f_e, p_u). \tag{2}$$

After ingestion, gametocytes develop into gametes and undergo fertilization to form zygotes which will develop into oocysts [54]. A female gametocyte only becomes a single female gamete while a male gametocyte produces a small number of male gametes via a replication process [6,7, 55]. However, not all male gametocytes ingested by mosquitoes undergo replication to produce male gametes [56], and some of the male gametes lack nuclei and are therefore not viable for fertilization [7]. Accordingly, the initial number of zygotes $Z(\tau = 0)$ is modeled by a binomial distribution:

$$Z(\tau = 0) \sim \mathrm{Bin}(\min(p_g \alpha M, F), p_f), \tag{3}$$

where p_g is the fraction of male gametocytes that are able to produce male gametes via repli-

cation, α is the number of male gametes that are produced by male gametocytes and viable for fertilization and p_f is the probability of successful fertilization. Since p_g and α are structurally non-identifiable, we define $\rho = p_g\alpha$, which represents the ratio of the number of viable male gametes to the number of male gametocytes ingested by the mosquito (i.e., the male gamete-to-gametocyte ratio). After determining the initial number of zygotes $Z(\tau = 0)$ post feeding, for each of the zygotes z_k ($k \in \{1, 2, ..., N\}$, $K = Z(0)$), the process of the development from zygote to oocyst O and subsequently sporozoite S is modeled using an individual based model. For each zygote z_k, transition times are sampled by randomly generating the transition times individually. The number of oocysts $O(\tau)$ at time τ post feeding is modeled by:

$$O(\tau) = \Sigma_{k=1}^{K} \Phi_O(k, \tau), \tag{4}$$

where

$$\Phi_O(k, \tau) = \begin{cases} 1, & \tau'_k \leq \tau < \tau'_k + \tau''_k \\ 0, & \text{otherwise} \end{cases} . \tag{5}$$

In Eq. 5, τ'_k is the transition time from Z to O for the kth zygote, sampled from a gamma distribution $\Gamma(\alpha_{ZO}, \beta_{ZO})$, with mean α_{ZO}/β_{ZO}, τ''_k is the transition time from O to S for the kth zygote, sampled from a gamma distribution $\Gamma(\alpha_{OS}, \beta_{OS})$, with mean α_{OS}/β_{OS}, where α_{ZO} and α_{OS} are the shape parameters and β_{ZO} and β_{OS} are the rate parameters of the gamma distributions. Since the probability of human-to-mosquito transmission depends only on the presence of oocysts or sporozoites, rather than their abundance, an indicator function was used to represent the infected status of the mosquito:

$$\mathbf{1}_O(\tau) = \begin{cases} 1, & O(\tau) > 0 \\ 0, & O(\tau) = 0 \end{cases} . \tag{6}$$

The parameter values of gamma distributions $\Gamma(\alpha_{ZO}, \beta_{ZO})$ and $\Gamma(\alpha_{OS}, \beta_{OS})$, which determine the times of transition between different states, are provided by [25]. Note that the mosquito-to-human transmission probability does depend on the abundance of sporozoites [57] and so future work that considered the entire transmission process would require a (straightforward) extension to this aspect of the within-mosquito model.

Simulation of mosquito feeding assays and calculation of the human-to-mosquito transmission probability

This section describes the procedure for simulating a direct feeding assay in which N_M mosquitoes are brought into contact with an infected human whose peripheral blood contains G_M male gametocytes and G_F female gametocytes. Since the duration of mosquito feeding in the experiments is generally less than a few hours, it is reasonable to assume that gametocyte concentration in the human bloodstream does not vary during the feeding period.

The numbers of male and female gametocytes ingested by each of the N_M mosquitoes were simulated using Eqs. 1 and 2. For each mosquito, Eq. 3 was used to calculate the initial number of zygotes $Z(0)$. The mosquito is considered to be infected if it has at least one zygote $Z(0) \geq 1$. Eqs. 4–6 were used to simulate the times when oocysts or sporozoites are first presented in each mosquito. The mosquito is infected at time τ if it has developed oocysts, i.e., $\mathbf{1}_O(\tau) = 1$.

Mosquitoes may die during the mosquito feeding assay. To account for the effect of mosquito infection status on mosquito death, a Gompertz function of time τ was proposed to model the mosquito death rate μ_M. The parameters governing the Gompertz function were estimated using experimental data provided in [25] (details about the function and data fitting are provided in the S1 Appendix).

The time of death t'_n for the nth mosquito is determined by solving

$$p'_n = e^{\int_0^{t'_n} \mu_M(\tau) d\tau} \tag{7}$$

for t'_n, where p'_n is a random number sampled from a uniform distribution $U[0, 1]$. After computing the death time t'_n for each of the N_M mosquitoes, whether the nth mosquito survives for a duration τ post feeding is determined by:

$$L_n(\tau) = \begin{cases} 1, & \text{if } t'_n > \tau \\ 0, & \text{otherwise} \end{cases} . \tag{8}$$

With the mortality status of each of the mosquitoes determined, the proportion of surviving mosquitoes with developed oocysts (P_e) is given by:

$$P_e = \frac{\sum_{n=1}^{N_M} \mathbf{1}_{O,n}(\tau = 8.5) L_n(\tau = 8.5)}{\sum_{n=1}^{N_M} L_n(\tau = 8.5)}, \tag{9}$$

where the choice of $\tau = 8.5$ days is based on the detection time of oocysts in the VIS data [11]. P_e will be fitted to the direct feeding assay data in the VIS [11] to estimate several biological parameters, and the details about the data and fitting methods will be provided in the following sections.

Parameters of the mosquito feeding model

All parameters of the mosquito feeding model are listed in Table 1. The value for the blood meal volume taken by a mosquito (V) is obtained based on [58]. The value of the fraction of total human blood volume localized to the site of a mosquito bite (f_e) is set to 0.00025, which corresponds to 1mL localized to the site of mosquito bite. Note that the value of f_e should be much larger than V/V_H (i.e., the sampling pool of the binomial distribution is equal to the blood volume V if $f_e = V/V_H$) to retain stochasticity in the sampling process while also be much smaller than 1 (i.e., the sampling pool of the binomial distribution is the human blood volume V_H) as a mosquito blood meal is a localized event and cannot capture any gametocyte circulating in the human blood stream with equal probability. We assume the mosquito bite volume V is 3.4μL [58] and the human blood volume V_H is 4000mL. The expected value for the number of gametocytes taken in the blood meal by mosquitoes is independent of f_e and the variance only very weakly dependent on f_e. Hence our model is highly insensitive to the choice of f_e (see S8 Fig). The values of the parameters governing the gamma distributions of the transition time between Z to O and O to S (i.e., α_{ZO}, β_{ZO}, α_{OS} and β_{OS}) are chosen from [25], such that the mean transition time for zygotes to oocysts is 3.4 days and the mean transition time from oocysts to sporozoites is 9.2 days. Estimates for the male gamete-to-gametocyte ratio ρ and the probability of successful fertilization for each pair of gametes p_f are not available in the literature, and are key parameters that we estimate through our Bayesian inference procedure. The death rates of mosquitoes (μ_M) is estimated by fitting a Gompertz function to mosquito survival data (see S1 Appendix).

Model fitting

To estimate the male gamete-to-gametocyte ratio ρ and the probability of successful fertilization p_f, the mosquito feeding model was fitted to the direct feeding assay data from a previously published VIS [11] using an approximate Bayesian computation sequential Monte Carlo (ABC-SMC) algorithm [59]. The data used in the model fitting includes the male and female gametocytemia

Table 1: **Parameters for the mosquito feeding model.**

Parameter	Description	Unit	Value	Reference
f_e	Fraction of total human blood volume localized to the site of a mosquito bite	(unitless)	0.00025	See the main text
V	Blood meal volume taken by mosquito	μL	3.4	[58]
ρ	male gamete-to-gametocyte ratio	(unitless)	0.80	Estimated
p_f	Probability of successful fertilization for each pair of viable gametes	(unitless)	0.029	Estimated
α_{ZO}	Shape parameter of gamma distribution for transition from Z to O	(unitless)	13.8	[25]
β_{ZO}	Rate parameter of gamma distribution for transition from Z to O	(unitless)	3.9	[25]
α_{OS}	Shape parameter of gamma distribution for transition from O to S	(unitless)	19.3	[25]
β_{OS}	Rate parameter of gamma distribution for transition from O to S	(unitless)	2.1	[25]
τ	Time for detecting oocysts post feeding	Day	8.5	[11]
μ_M	The death rate of mosquitoes	Function of time		Estimated

($G_M f_e$ and $G_F f_e$ in Eqs. 1 and 2) in 11 volunteers and the proportion of mosquitoes developing oocysts (P_e in Eq. 9), which are provided in S1 Fig and S2 Fig. Data from all volunteers were pooled for model fitting (rather than evaluated using hierarchical modeling), because the parameters to be estimated are not influenced by between-volunteer variance. Moreover, there are no data imbalance issues because each volunteer contributes the same number of observations (three data points).

In the ABC-SMC method, the posterior distribution is approximated by comparing the distance between simulated and observed data, with parameter samples initially drawn from the prior distribution and then from a sequence of intermediate distributions, progressively refined using sequential Monte Carlo, and with tolerance gradually decreasing over generations [59]. The prior distributions of ρ and p_f must be defined first. To inform the prior distribution for ρ, we consider that $\rho = p_g \alpha$, where p_g represents the fraction of male gametocytes undergoing replication to produce male gametes and α is the mean number of viable male gametes produced per male gametocytes undergoing replication. There is substantial uncertainty surrounding the value of p_g, with experimental studies reporting values spanning the full range from 0 to 1 [56,60]. For α, it is known that each male gametocyte undergoing replication gives rise to 8 male gametes [6], but not all of these are viable, as only gametes containing a nucleus are capable of fertilization [7].

Given that at least one nucleus is present per gametocyte, the plausible biological range for α is between 1 and 8. Accordingly, the prior distribution for ρ is given by $U[0,1] \times U[1,8]$ (see S2 Appendix). For p_f, where limited empirical information is available, a uniform prior distribution $U[0,1]$ was chosen, allowing the data to inform the posterior distribution.

In the first generation of the ABC-SMC algorithm, after specifying the prior distributions, the parameters ρ and p_f are sampled independently from prior distributions. In subsequent generations, ρ and p_f are sampled from the intermediate posterior distributions. For each parameter sample (ρ, p_f), simulated data $\{P'_{e,1}, \ldots, P'_{e,11}\}$ are generated for the 11 volunteers by using Eqs. 1–9. The Euclidean distance d between the simulated data $\{P'_{e,1}, \ldots, P'_{e,11}\}$ and observed data $\{P_{e,1}, \ldots, P_{e,11}\}$ is given by:

$$d = \left[\sum_{i=1}^{11} \left(P'_{e,i} - P_{e,i} \right)^2 \right]^{1/2}, \tag{10}$$

which is a common choice of distance metric (see [61] for details). The sampling process is repeated until 5000 samples are accepted in each generation. The algorithm terminates when the acceptance rate falls below 0.5%, which serves as the stopping rule [62]. Full details of the ABC-SMC implementation, including the choice of tolerance, resampling and weighting, and pseudo-code, are provided in S2 Appendix. The results of model fitting for all 11 volunteers are provided in S2 Fig. Fitting results include the joint posterior distribution of ρ and p_f and the relationship between the proportion of mosquitoes developing oocysts and male and female gametocytes generated by 5000 model simulations based on 5000 samples from the posterior parameter distribution (Fig. 2).

A model of within-human parasite dynamics

Here we introduce a new model of within-human parasite dynamics that is integrated with the mosquito feeding model to form the multi-scale human-to-mosquito transmission model. The within-human parasite dynamics model was developed by extending a previously developed gametocyte dynamics model [19,20] to capture the development of female and male gametocytes. A schematic diagram of the new within-human parasite dynamics model is shown in Fig. 7. The model contains three major parasite populations: asexual parasites $P(a,t)$, sexually committed parasites $P_G(a,t)$ and gametocytes (including immature stages $G_1(t)$–$G_4(t)$ and mature male $G_M(t)$ and female $G_F(t)$ populations), where a represents parasite age and t represents time

since the onset of blood stage infection. Asexual parasites can invade red blood cells (RBCs) and initiate an asexual life cycle lasting a_L hours, during which they undergo maturation and replication. The parasitized RBCs (pRBC) may die at any time governed by a rate parameter δ_p. If they reach the end of the asexual life cycle, rupture occurs, releasing merozoites which invade uninfected RBCs and initiate a new replication cycle. During the asexual life cycle, a small fraction of the parasites (at age a_s) differentiate into sexually committed parasites and eventually develop into male and female gametocytes.

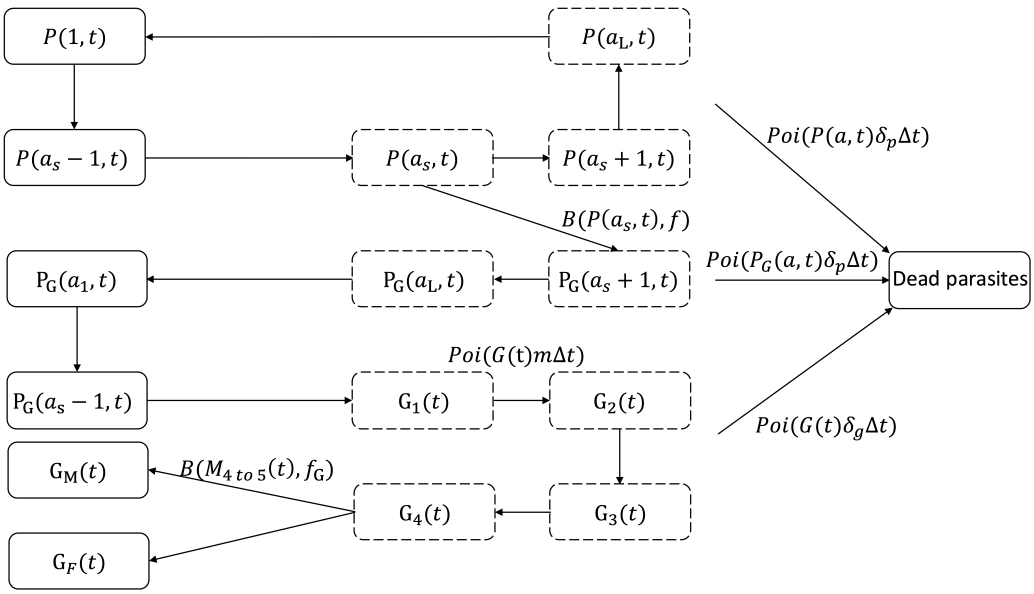

Figure 7: **A schematics diagram of the new within-human parasite dynamics model.** The model contains three major parasite populations: P (asexual parasites), P_G (sexually committed parasites) and G (gametocytes). P and P_G are functions of parasitemia with age a at time t. The loop $P(a,t)$ describes the synchronous waves of asexual replication and maturation in a_L hours. A small fraction f of asexual parasites enter the sexual development cycle when sexual commitment occurs at age a_s, developing into sequestered gametocytes $G_1(t)$–$G_4(t)$ and eventually becoming circulating mature male (G_M) and female (G_F) gametocytes, with probabilities f_G and $1-f_G$ respectively. Parasites may die at any point during the developmental process, following a Poisson process with a probability per unit time (i.e., per time step Δt of one hour) determined by $P(a,t)\delta_p\Delta t$ (for asexual parasites), $P_G(a,t)\delta_p\Delta t$ (for sexually committed parasites) and $G(t)\delta_g\Delta t$ (for gametocytes), where δ_p is the natural death rate of parasites and δ_g is the natural death rate of gametocytes. Compartments with a dashed boundary represent those for which parasites of a particular age are sequestered to tissues and thus not measurable by sampling peripheral blood, whereas parasitemia refers to the parasite density in compartments with solid boundaries.

The within-human parasite dynamics are described by a discrete-time stochastic model with a time step of $\Delta t = 1$ hour. A tau-leaping algorithm [63] was used to simulate this model. In detail, the total number of asexual parasites at the time of inoculation $P(a,0)$ was first

calculated by multiplying the initial density parameter P_{init} (see Table 2) by an assumed blood volume V_H of 4000mL. The total number of asexual parasites $P(a,0)$ was then distributed across the a_L age bins by generating $P(a,0)$ random samples from a truncated normal distribution $N_{[1,a_L]}(\mu,\sigma^2)$ and rounding the samples to the nearest integers. Subsequently, the number of asexual parasites changes according to the following equation:

$$P(a,t) = \begin{cases} P(a-1,t-1) - D_{a-1}, & a = 2,3,...,a_{s-1},a_{s+1},...,a_L \\ r_p\left[P(a_L,t-1) - D_{a_L}\right], & a = 1 \end{cases} \tag{11}$$

where a_L is the duration (in hours) of each asexual replication cycle, a_s is the age at which sexual commitment occurs, r_p is the parasite replication number indicating the average number of newly infected RBCs attributable to the rupture of a single infected RBC. Note that the parasite replication number r_p is different from the so-called parasite multiplication rate, the latter of which is a 'net replication rate' quantified by the increase in parasite numbers due to replication (r_p) and the decrease due to parasite death or sexual commitment. Parasite multiplication rate is calculated by $r_p\exp(1-\delta_p\Delta t)^{a_L/\Delta t}(1-f)$, where the term $(1-\delta_p\Delta t)^{a_L/\Delta t}(1-f)$ gives the fraction of surviving asexual parasites after death and sexual conversion per replication cycle (see S3 Appendix for the details), δ_p is the rate of natural death of asexual parasites and f is the probability of sexual commitment for each parasite. The number of asexual parasites that die D_a during each time step ($\Delta t = 1$h) is sampled from a Poisson distribution $\mathrm{Poi}(P(a-1,t-1)\delta_p\Delta t)$. For those parasites that may undergo sexual commitment (i.e., parasites with age a_s):

$$\begin{cases} P(a_s+1,t) = P(a_s,t-1) - D_{a_s} - B, \\ P_G(a_s+1,t) = B, \end{cases} \tag{12}$$

where B represents the number of parasites that become sexually-committed, sampled from a binomial distribution $\mathrm{Bin}(P(a_s,t-1)-D_{a_s},f)$ where f is the probability of sexual commitment for each parasite and is assumed to be fixed over the course of infection. The first line of Eq. 12 captures the evolution of the parasites remaining in the asexual life cycle, while the second line of Eq. 12 describes the number of parasites undergoing sexual commitment. Sexually committed

parasites continue the rest of the replication cycle, which is modeled by:

$$P_G(a,t) = \begin{cases} P_G(a-1,t-1) - D_{P_G,a-1}, & a = 2,3,...,a_{s-1},a_{s+1},...,a_L \\ r_p\left[P_G(a_L,t-1) - D_{P_G,a_L}\right], & a = 1 \end{cases} \tag{13}$$

where $D_{P_G,a}$ represents the number of sexually-committed parasites that die in each time step, sampled from $\text{Poi}(P_G(a,t-1)\delta_p\Delta t)$. The sexually committed parasites will develop into immature gametocyte stages (G_1–G_4) and eventually mature male gametocytes G_M and female gametocytes G_F, both of which circulate in the bloodstream. The dynamics of the gametocytes $G_1 - G_4$ are modeled by:

$$\begin{cases} G_1(t) = P_G(a_s-1,t-1) - D_{P_G,a_s-1} + G_1(t-1) - D_{G_1} - M_{1\,to\,2}, \\ G_i(t) = G_i(t-1) + M_{i-1\,to\,i} - D_{G_i} - M_{i\,to\,i+1}, \quad i = 2,3,4 \end{cases} \tag{14}$$

where D_{G_i} represents the number of dead stage i gametocytes, sampled from $\text{Poi}(G_i(t-1)\delta_g\Delta t)$, where δ_g is the death rate of immature gametocytes and $M_{i\,to\,i+1}$ represents the number of stage i gametocytes maturing to become stage $i+1$ gametocytes, sampled from $\text{Poi}(G_i(t-1)m\Delta t)$ for $i = 1,2,3,4$, where m is the rate of gametocyte maturation. Male and female gametocytes develop after stage IV [2] and their dynamics are modeled by:

$$\begin{cases} G_M(t) = G_M(t-1) - D_M + B_M, \\ G_F(t) = G_F(t-1) - D_F + B_F, \end{cases} \tag{15}$$

where D_M represents the number of dying male gametocytes during a time step, sampled from $\text{Poi}(G_M(t-1)\delta_{gc})$, where δ_{gc} is the death rate of circulating gametocytes. Similarly, D_F represents the number of dying female gametocytes during a time step, sampled from $\text{Poi}(G_F(t-1)\delta_{gc})$, B_M represents the number of immature gametocytes that become male gametocytes, sampled from $\text{Bin}(M_{4\,to\,5}, f_G)$, where f_G is the probability that a sequestered G_4 gametocyte develops into a male gametocyte, referred to as the male gametocyte fraction, and B_F represents the number of immature gametocytes that become female gametocytes, given by $M_{4\,to\,5} - B_M$.

To simulate asymptomatic infections, the parasite replication number was adjusted to be

$$r_p = 1/(1-\delta_p\Delta t)^{42/\Delta t}/(1-f) \tag{16}$$

such that the PMR is equal to 1 at the specified set-point parasitemia level (i.e., 10^4 and 10^6), which yields cyclical asexual parasitemia around the set-point level, mimicking an active immune response.

Methods for sensitivity analysis

To quantify the correlations between various host factors and the human-to-mosquito transmission probability of asymptomatic infections, a partial rank correlation coefficient (PRCC) analysis was conducted. The PRCC analysis is designed to identify the correlation of two variables after removing any linear dependence on all other variables in a model with multiple parameters [36]. In detail, Latin Hypercube Sampling (LHS) was used to generate 1000 parameter sets by sampling from joint uniform distributions, with each parameter varied within $\pm 50\%$ of its benchmark value (see Table 1 and Table 2). For each parameter set, the within-human parasite dynamics model was simulated to generate the time series of gametocytemia of asymptomatic infections. At each time point, the male and female gametocyte density were used as inputs in the mosquito feeding model to compute the human-to-mosquito transmission probability defined as the proportion of surviving mosquitoes with developed oocysts (P_e). After obtaining the time series of the transmission probability, $t_{0.001}$ and p_{60} were calculated. The results of the analysis include the PRCC values between $t_{0.001}$ and the parameters shown in Fig. 4, as well as between p_{60} and the same parameters.

Parameters of the within-human parasite dynamics model

All parameters of the within-human parasite dynamics model are listed in Table 2. The parameter values for the within-human parasite dynamics model are chosen from the population-level estimates reported in [19], where a gametocyte dynamics model was fitted to the VIS data [11]. The SD of the initial age distribution (σ) is instead taken from [64], as volunteers in the VIS were inoculated with predominantly early ring–stage parasites, resulting in a tighter parasite age distribution than in natural infections. The value of the male gametocyte fraction (f_G) is chosen from [11, 65].

All the parameters of the within-human parasite dynamics model are included in the partial rank correlation coefficient (PRCC) sensitivity analysis, except for the sequestration age of asexual parasites a_s and the length of the replication cycle of asexual parasites a_L. For the parameters of mosquito feeding model, the blood meal volume taken by mosquito V, the male gamete-to-

gametocyte ratio ρ and the probability of successful fertilization for each pair of viable gametes p_f, are included in the PRCC sensitivity analysis (see Table 1).

Table 2: **Parameters for the within-human parasite dynamics model.**

Parameter	Description	Unit	Value	Reference
P_{init}	Inoculation concentration	parasite/mL	0.08	[19]
μ	Mean of the initial age distribution	h	7	[19]
σ	SD of the initial age distribution	h	8	[64]
r_p	Replication number	(unitless)	71	[19]
f	Fraction of parasites entering sexual development	(unitless)	0.006	[19]
δ_p	Death rate of asexual and sexual parasites	h^{-1}	0.03	[19]
δ_g	Death rate of sequestered gametocytes	h^{-1}	0.0004	[19]
δ_{gc}	Death rate of circulating gametocytes	h^{-1}	0.007	[19]
m	Maturation rate of gametocytes	h^{-1}	0.02	[19]
f_G	Male gametocyte fraction	(unitless)	0.2	[11, 65]
a_s	Sequestration age of asexual parasites	h	25	[19]
a_L	Length of life cycle of asexual parasites	h	42	[19]

Data availability

Data were obtained from previously published studies [11]. The processed data used for model fitting are available at https://github.com/XSSUN2/Modelling-the-transmission-of-malaria-parasites-from-a-human-host-to-mosquitoes.git.

Code availability

All the code used for model analysis and result visualization is publicly available at https://github.com/XSSUN2/Modelling-the-transmission-of-malaria-parasites-from-a-human-host-to-mosquitoes.git. All analyses were performed in R (version 4.2.1).

Acknowledgments

We thank the Australian Research Council (ARC) for supporting this research through a Discovery Project (DP210101920) and a Laureate Fellowship awarded to JMM (FL240100126) which support XS, PC and JMM. We thank Medicines for Malaria Venture for funding the VIS clinical

trials. JSM is supported by an NHMRC Investigator Grant (2016396). Computer simulations were conducted on the Nectar Research Cloud, a collaborative Australian research platform supported by the National Collaborative Research Infrastructure Strategy (NCRIS).

Author contributions

X.S., M.W.A.D., J.S.M., J.M.M. and P.C. contributed to conceptualization. M.W.A.D. and J.S.M. contributed to data curation. X.S. contributed to formal analysis. X.S., J.M.M. and P.C. contributed to methodology. J.M.M. and P.C. contributed to supervision. X.S. contributed to visualization. X.S., J.M.M. and P.C. contributed to writing of the original draft. X.S., M.W.A.D., J.S.M., J.M.M. and P.C. contributed to review and editing of the manuscript.

Competing interests

JSM was funded by Medicines for Malaria Venture to run the VIS clinical trials.

Supplementary materials

S1 Appendix.

Estimation of death rate of mosquitoes. Previous analyses on mosquito survival have revealed that a Gompertz function provides an excellent fit to data. Mortality rates generally increase with age for mosquitoes [25, 52, 66]. In our model, the death rate μ is assumed to be a Gompertz function of time τ. We allow for a potential difference between infected ($E = 1$) and uninfected ($E = 0$) mosquitoes:

$$\mu_M(\tau) = ae^{b\tau + cE}, \tag{17}$$

where a, b and c are non-zero constants. The mosquito survival $p(\tau)$ is then given by the following differential equation:

$$\frac{dp}{d\tau} = -\mu_m p \tag{18}$$

To solve this, we separate the variables and integrate both sides:

$$\int \frac{1}{p}\, dp = \int -ae^{b\tau + cE}\, d\tau \tag{19}$$

The equation integrates to:

$$\ln p(\tau) = -\frac{a}{b} e^{b\tau + cE} + C$$

Substitute $p(0) = 1$:

$$C = \frac{a}{b} e^{cE}$$

Finally, we get the solution:

$$p(\tau) = e^{-\frac{a}{b} e^{cE}(e^{b\tau} - 1)} \tag{20}$$

We fit this equation to mosquito survival data (at 27°C in [25]) by using nonlinear least squares estimation *nlsLM* in package *minpack.lm* (with default settings) in R (version 4.2.1). Results are shown in the Figure below.

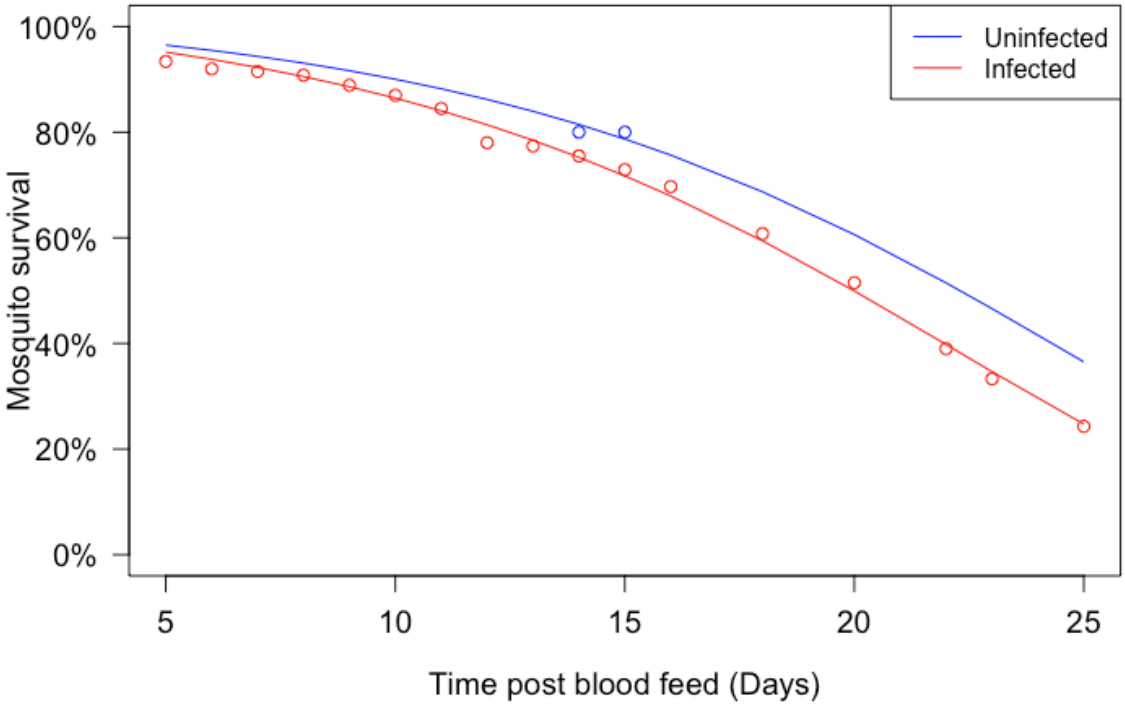

Fitting results for the death rate of mosquitoes μ_M. The dots represent the data for infected mosquitoes (red) and uninfected mosquitoes (blue). The curves are the fitting results for the death rate μ_M (infected $E = 1$, red, and uninfected $E = 0$, blue).

S2 Appendix.

Methods for estimating biological parameters. To calculate the density of the prior distribution of ρ, $U[0,1] \times U[1,8]$, we employ the probability density function (PDF) transformation method. Let $X \sim U[0,1]$ and $Y \sim U[1,8]$, and define $Z = XY$. the individual PDFs of X and Y are:

$$f_X(x) = 1, for\ x \in [0,1], \tag{21}$$

$$f_Y(y) = \frac{1}{7}, for\ y \in [1,8]. \tag{22}$$

Since X and Y are independent, the joint PDF of X and Y, denoted by $f_{X,Y}(x,y)$, is:

$$f_{X,Y}(x,y) = f_X(x)f_Y(y) = 1 \times \frac{1}{7} = \frac{1}{7}, for\ x \in [0,1], y \in [1,8]. \tag{23}$$

We are interested in the distribution of $Z = XY$. To derive $f_Z(z)$, we apply the change-of-

variable technique, where the Jacobian determinant is:

$$J = \frac{\partial(z,x)}{\partial(x,y)} = \begin{bmatrix} \frac{\partial z}{\partial x} & \frac{\partial z}{\partial y} \\ \frac{\partial x}{\partial x} & \frac{\partial x}{\partial y} \end{bmatrix} = \begin{bmatrix} y & x \\ 1 & 0 \end{bmatrix} \Rightarrow det(J) = -x. \tag{24}$$

Using this transformation, the PDF of Z is given by:

$$f_Z(z) = \int f_{Z,X}(z,x)dx = \int f_{X,Y}(x,y) \cdot |\frac{\partial(x,y)}{\partial(z,x)}|dx = \int f_{X,Y}(x,y) \cdot |\frac{1}{det(J)}|dx. \tag{25}$$

Since $Y = \frac{z}{x} \in [1,8]$, it follows that $x \in [z/8, min(z,1)]$, and the PDF of Z becomes:

$$f_Z(z) = \int_{x=z/8}^{min(z,1)} f_X(x) f_Y(\frac{z}{x}) \frac{1}{|x|} dx. \tag{26}$$

For $z \in [0,1]$, the PDF is:

$$f_Z(z) = \int_{x=z/8}^{z} \frac{1}{7} \cdot \frac{1}{x} dx = \frac{1}{7} ln8. \tag{27}$$

For $z \in (1,8]$, the PDF is:

$$f_Z(z) = \int_{x=z/8}^{1} \frac{1}{7} \cdot \frac{1}{x} dx = \frac{1}{7} ln(\frac{8}{z}). \tag{28}$$

Therefore, the PDF of Z is:

$$f_Z(z) = \begin{cases} \frac{1}{7} ln8 & z \in [0,1] \\ \\ \frac{1}{7} ln(\frac{8}{z}) & z \in (1,8] \end{cases}. \tag{29}$$

To perform the ABC-SMC, we independently sample the parameters ρ and p_f from prior distributions in the first generation ($g = 1$). For each parameter sample (ρ, p_f), simulated data $\{P'_{e,1}, \ldots, P'_{e,11}\}$ are generated for the 11 volunteers. We then compute the Euclidean distance d, which is a common choice of distance metric (see [61] for details), between the simulated data $\{P'_{e,1}, \ldots, P'_{e,11}\}$ and observed data $\{P_{e,1}, \ldots, P_{e,11}\}$, as follows:

$$d = \left[\sum_{i=1}^{11} \left(P'_{e,i} - P_{e,i} \right)^2 \right]^{1/2}. \tag{30}$$

The sampled parameter pairs (ρ, p_f) are accepted in the first generation if $d < \epsilon_1$, where

$\epsilon_1 = \sum_{i=1}^{11}(P'_{e,i} - P_{e,i})^2]^{1/2}$ represents the 'data-only' distance. We repeat the sampling process until $L = 5000$ samples $\{(\rho, p_f)_l^{g=1}\}_{l=1}^L$ are obtained and assigned an equal normalized weight to each accepted sample $w_l^{g=1} = 1/L$. For subsequent generations, new samples $(\rho, p_f)^*$ are drawn from the weighted empirical distribution of accepted samples from the previous generation, $\{(\rho, p_f)_l^{g-1}\}_{l=1}^L$, using weights $\{w_l^{g-1}\}_{l=1}^L$. Each sample is perturbed using a multivariate normal kernel $K[(\rho, p_f)|(\rho, p_f)^*]$, with mean and standard deviation set to be the sample mean and standard deviation of the accepted samples from the previous generation $g-1$ to improve sampling efficiency [67]. As in the first generation, simulated data are generated by the model for each perturbed sample (ρ, p_f) and the distance d between the simulated and observed data is calculated. (ρ, p_f) is accepted if $d < \epsilon_g$, where ϵ_g is given by:

$$\epsilon_g = \begin{cases} \left[\sum_{i=1}^{11}\left(P'_{e,i} - P_{e,i}\right)^2\right]^{1/2}, & if\ g = 1 \\ \text{Median}\left(\{d_n^{g-1}\}_{l=1}^L\right), & if\ g = 2, 3, \ldots, G \end{cases}. \tag{31}$$

The process is repeated until $L = 5000$ samples $\{(\rho, p_f)_l^g\}_{l=1}^L$ are accepted in each generation. The weights w^* for accepted samples are calculated using:

$$w^{*g}_k = \begin{cases} 1 & if\ g = 1 \\ \frac{\pi[(\alpha, p_f)_l^g]}{\Sigma_{j=1}^L w_j^{g-1} K[(\alpha, p_f)_k^g|(\alpha, p_f)_j^{g-1}]} & if\ g = 2, 3, \ldots, G \end{cases}. \tag{32}$$

where π denotes the prior distributions of ρ and p_f. After computing the weights, they are normalized, $w_l^g = w^{*g}_l/(\sum_{l=1}^L w^{*g}_n)$, so that $\sum_{l=1}^L w_l^g = 1$. The total number of generations G is determined by the acceptance rate of each generation, with the algorithm terminating once the acceptance rate drop below 0.5%, which serves as the stopping rule [62]. The algorithm terminated at $G = 8$ according to this stopping criterion. The parameter estimates for generations $G = 6$, 7 and 8 are shown below.

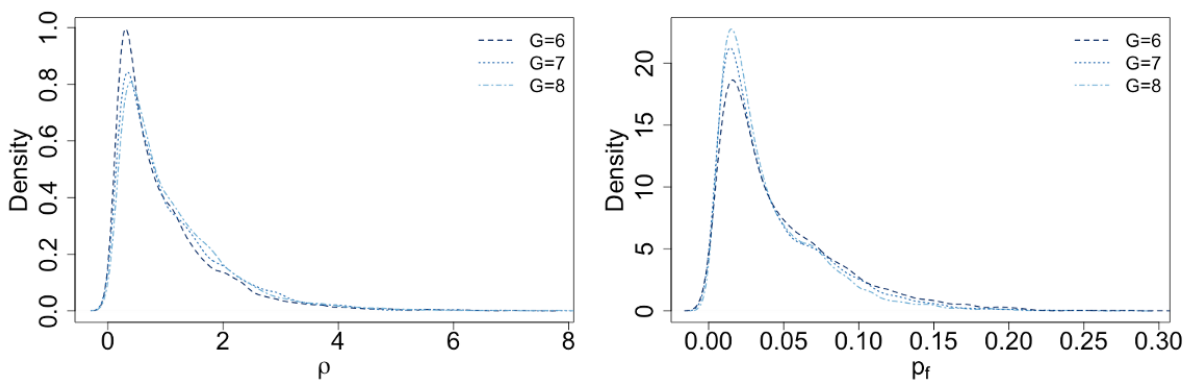

Marginal distributions of 5,000 draws from the posterior distribution for the male gamete-to-gametocyte ratio (ρ) and the probability of successful fertilization per gamete pair (p_f) across generations $G = 6$, 7, and 8, with colors from dark to light.

The pseudo-code for the algorithm is provided below.

Algorithm 1: Pseudo-code of ABC-SMC Algorithm

Input: Data $\{x_1, \cdots, x_n\}$

Output: $L = 5000$ posterior distribution samples $\{(\rho, p_f)_l\}_{l=1}^{L}$

Set the tolerance of the first generation $\epsilon_1 = [\sum_{i=1}^{11}(P_{e,i})^2]^{1/2}$

for *g=1,2,...,G* **do**

  for *l=1,2,...,L* **do**

    while $d_l^g > \epsilon_g$ **do**

      if *g=1* **then**

        Sample ρ^{**} and p_f^{**} independently from prior uniform distributions $U[0,1] \times U[1,8]$ and $U[0,1]$;

      else

        Sample $(\rho, p_f)^*$ from the last generation $\{(\rho, p_f)_l^{g-1}\}_{l=1}^{L}$ with weights $\{w_l^{g-1}\}_{l=1}^{L}$;

        Perturb the sample $(\rho, p_f)^{**} \sim K[(\rho, p_f)^{**}|(\rho, p_f)^*]$;

      end

      Using the model to generate simulated data $\{P'_{e,1}, \ldots, P'_{e,11}\}$ from $f(P_e|(\rho, p_f)^*)$;

      Calculate the distance between the simulated data $\{P'_{e,1}, \ldots, P'_{e,11}\}$ and the observed data $\{P_{e,1}, \ldots, P_{e,11}\}$, $d_l^g = [\sum_{i=1}^{11}(P'_{e,i} - P_{e,i})^2]^{1/2}$;

    end

    Set $(\rho, p_f)_l^g = (\rho, p_f)_l^{**}$ and calculate the weight for each of the accepted samples $w_l^g = \begin{cases} 1 & if\ g = 1 \\ \frac{\pi[(\rho,p_f)_l^g]}{\Sigma_{j=1}^{L} w_j^{g-1} K[(\rho,p_f)_l^g|(\rho,p_f)_j^{g-1}]} & otherwise \end{cases}$, where π is the prior distributions;

  end

  Normalize the weights $\{w_l^g\}_{l=1}^{L}$;

  Set the tolerance for the next generation $\epsilon_{g+1} = Median(\{d_l^g\}_{l=1}^{L})$;

end

S3 Appendix

Method for calculating of parasite multiplication rate. Consider a death process with death rate δ_p with population size P and a single time step $\Delta t = 1$ hour. Under one-step Tau-leaping, the number of deaths D during the step is sampled as

$$D \sim \mathrm{Poi}(P\delta_p \Delta t). \tag{33}$$

Define the (random) one-step survival fraction under Tau-leaping by

$$S = \frac{P - D}{P} = 1 - \frac{D}{P}. \tag{34}$$

Taking expectation and using linearity of expectation gives

$$\mathbb{E}[S] = \mathbb{E}\left[1 - \frac{D}{P}\right] = 1 - \frac{1}{P}\,\mathbb{E}[D]. \tag{35}$$

For a Poisson random variable, $\mathbb{E}[D] = P\delta_p \Delta t$, hence

$$\mathbb{E}[S] = 1 - \frac{1}{P}\,(P\delta_p \Delta t) = 1 - \delta_p \Delta t. \tag{36}$$

Now define a new death rate δ_p^* by matching the continuous-time exponential survival probability over one time step to the mean Tau-leaping survival fraction:

$$e^{-\delta_p^* \Delta t} \;=\; \mathbb{E}[S] = 1 - \delta_p \Delta t. \tag{37}$$

and therefore

$$\delta_p^* = -\frac{1}{\Delta t}\ln(1 - \delta_p \Delta t), 0 < \delta_p \Delta t < 1. \tag{38}$$

The multiplication rate is PMR $= r_p exp(-\delta_p^* a_L)(1 - f) = r_p exp(1 - \delta_p \Delta t)^{a_L/\Delta t}(1 - f)$.

713 **S1 Fig.**

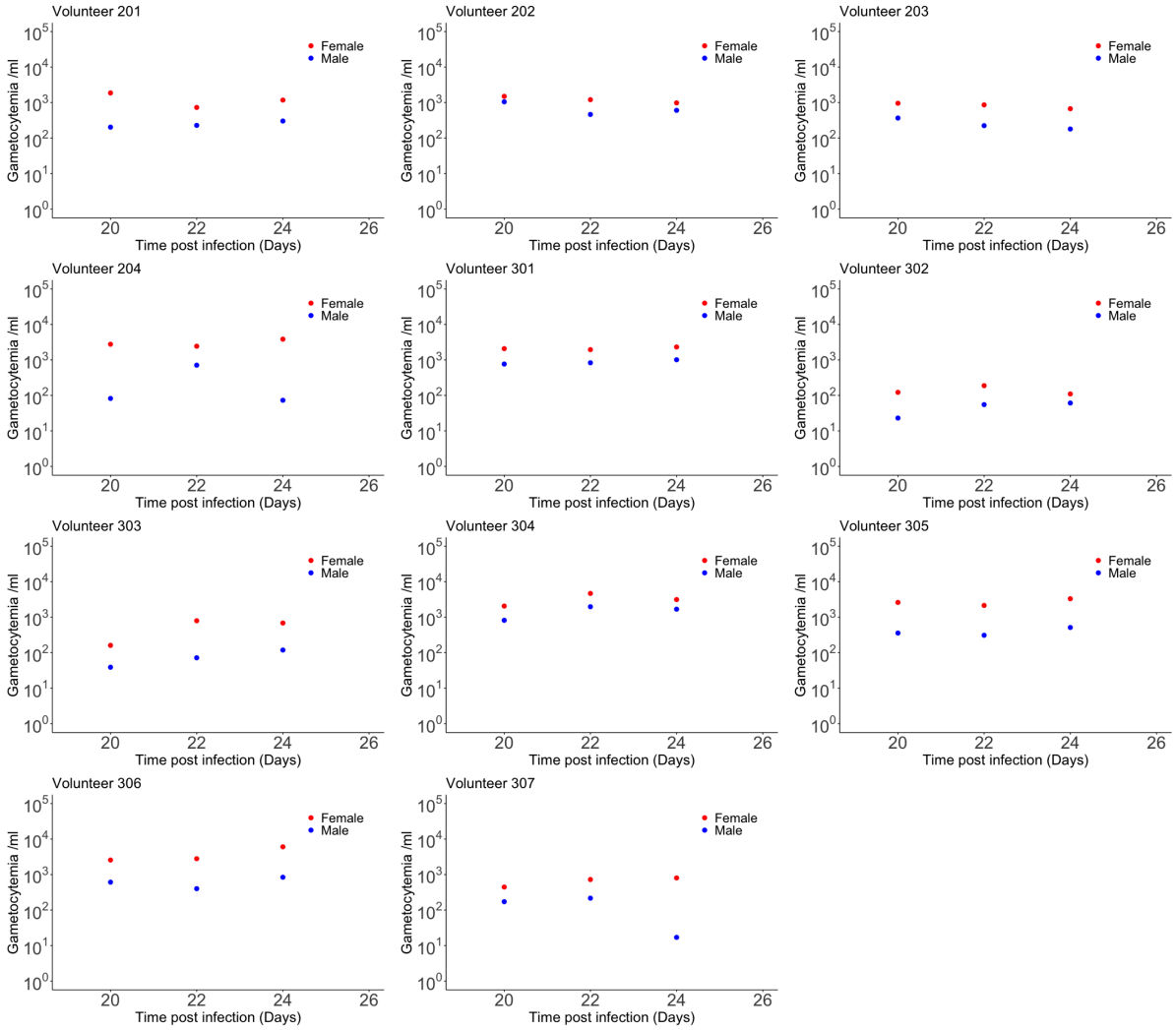

714

715 **Direct feeding assay data including male (blue dots) and female (red dots) game-**

716 **tocytemia for all 11 volunteers.**

S2 Fig.

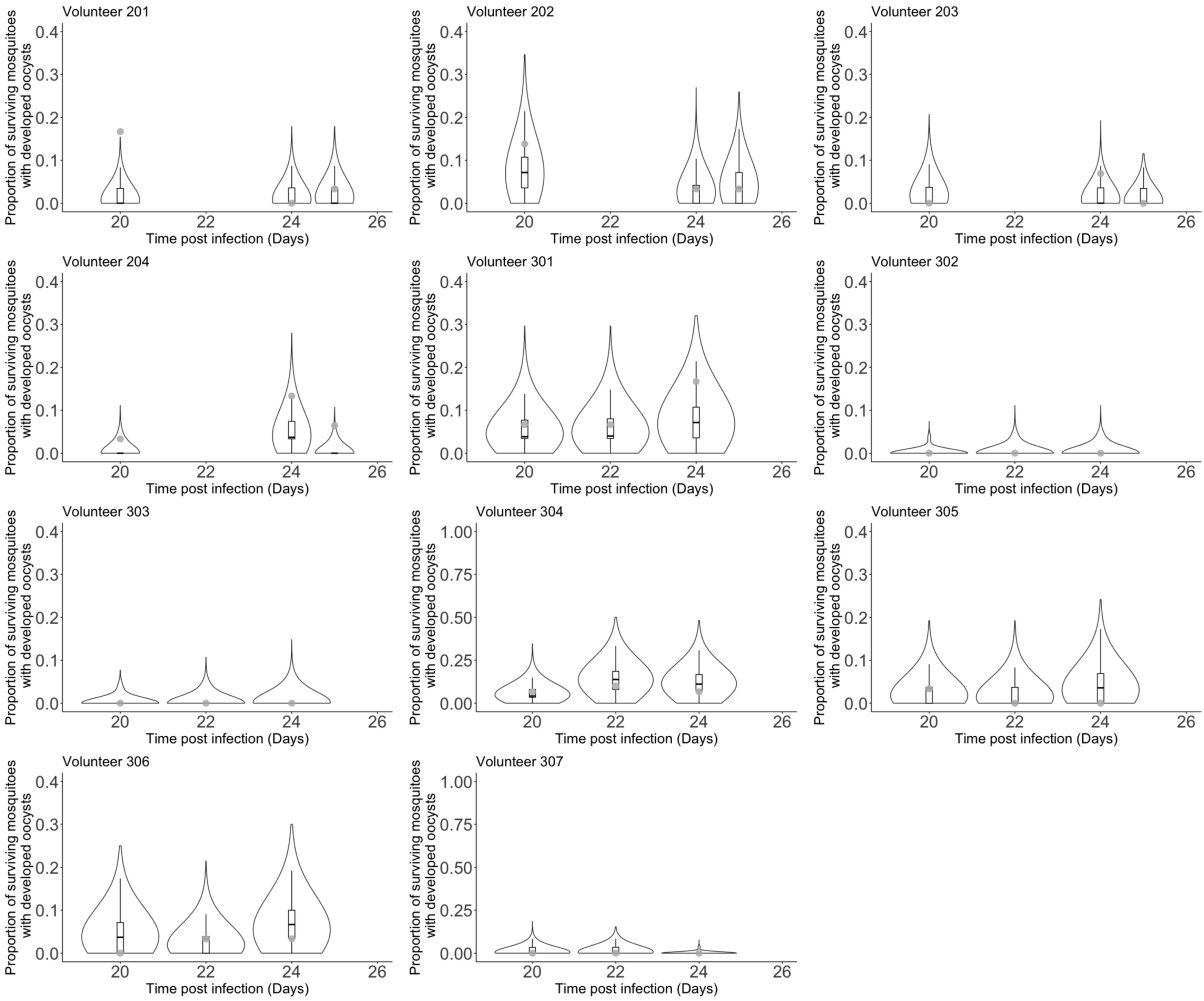

Results of model fitting for all 11 volunteers. Data are presented by grey dots. The violin plots show the 5000 predictions of fraction of surviving mosquitoes with developed oocysts generated by 5000 posterior samples. Box plots show the 25%, 50% (median) and 75% quantiles.

S3 Fig.

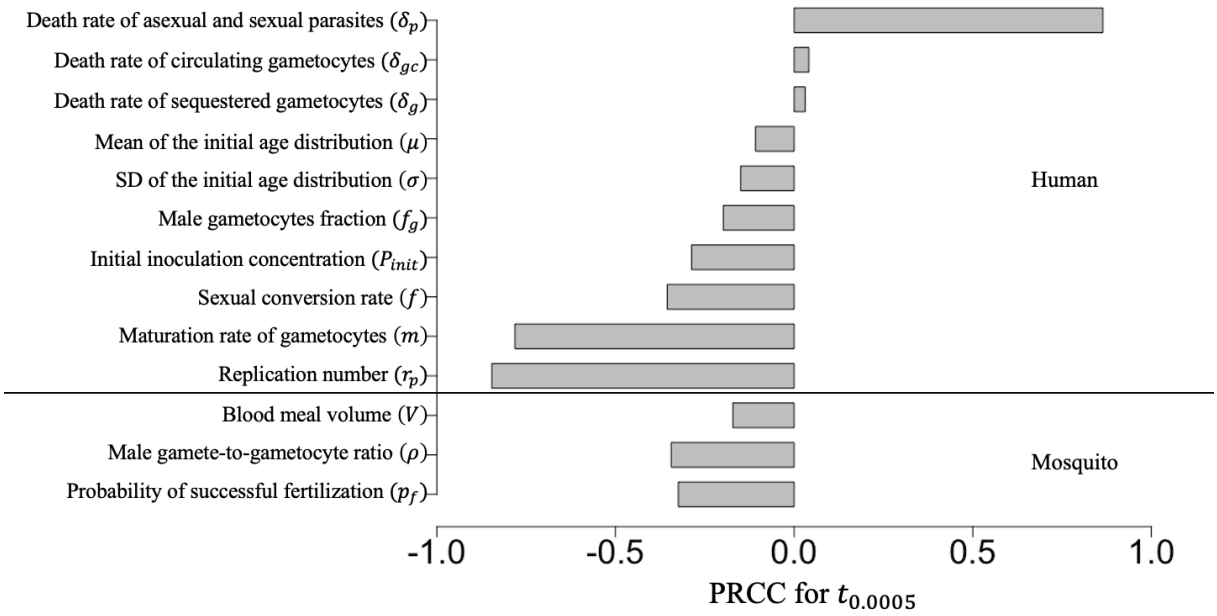

PRCC results between parameters and $t_{0.0005}$ for high transmission settings.

S4 Fig.

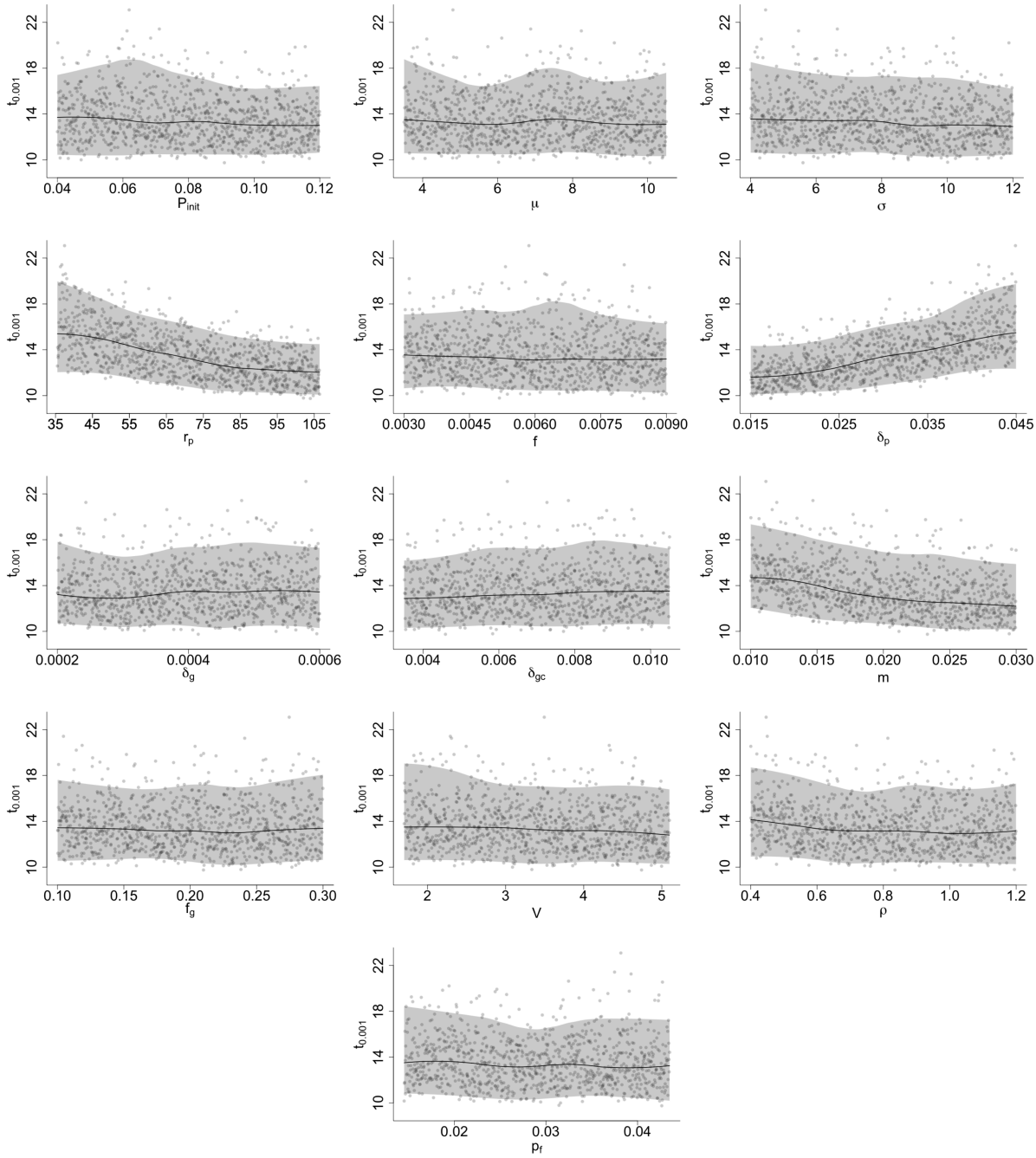

Marginal relationships between the LHS-sampled parameters and $t_{0.001}$.

S5 Fig.

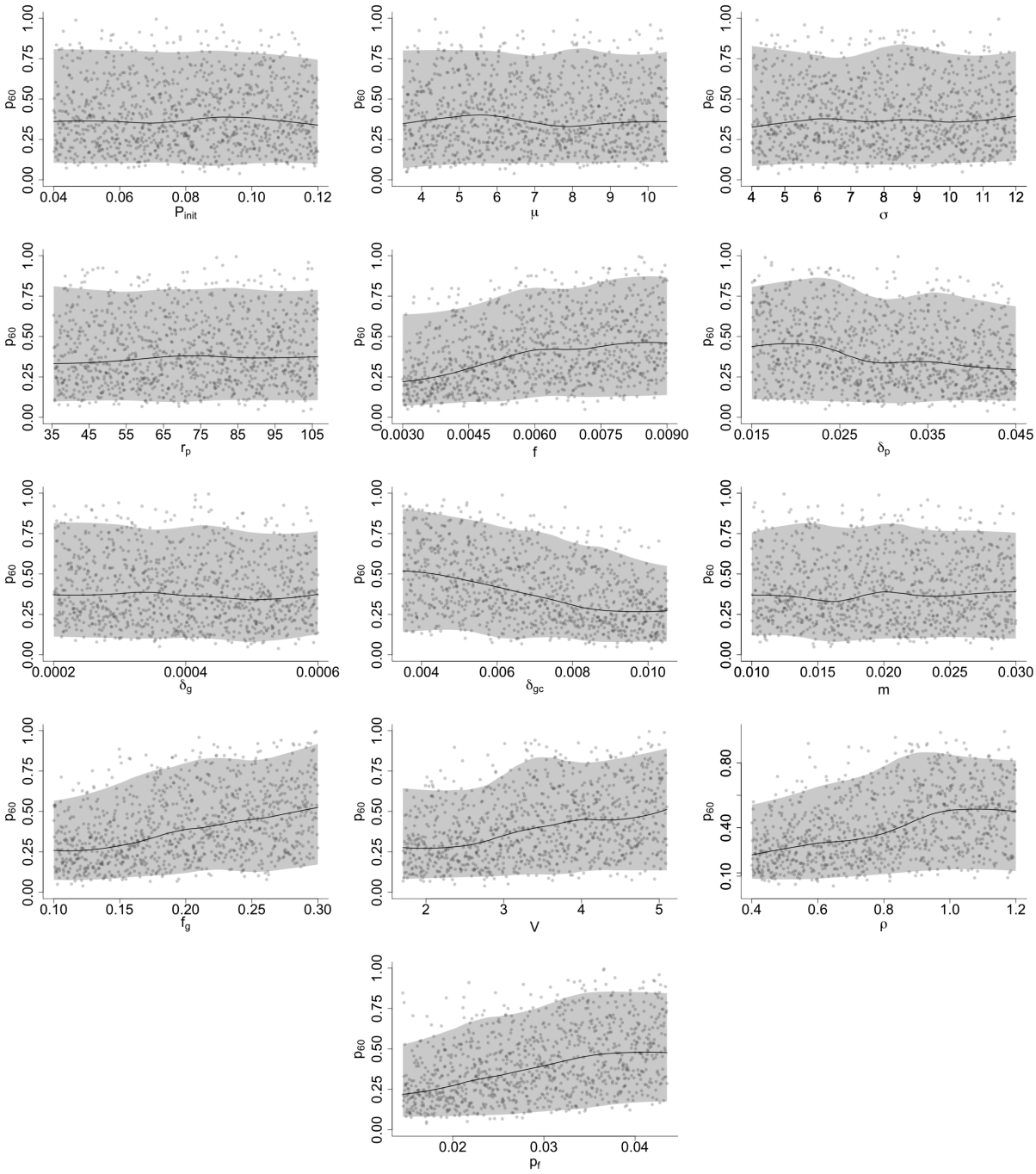

Marginal relationships between the LHS-sampled parameters and p_{60}.

S6 Fig.

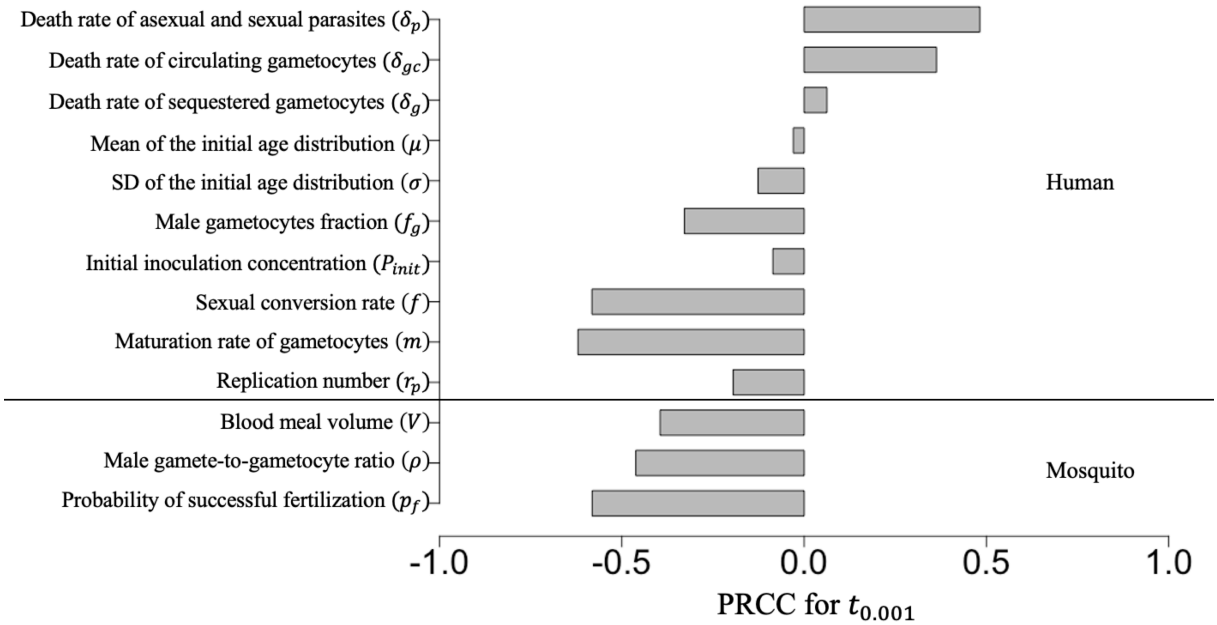

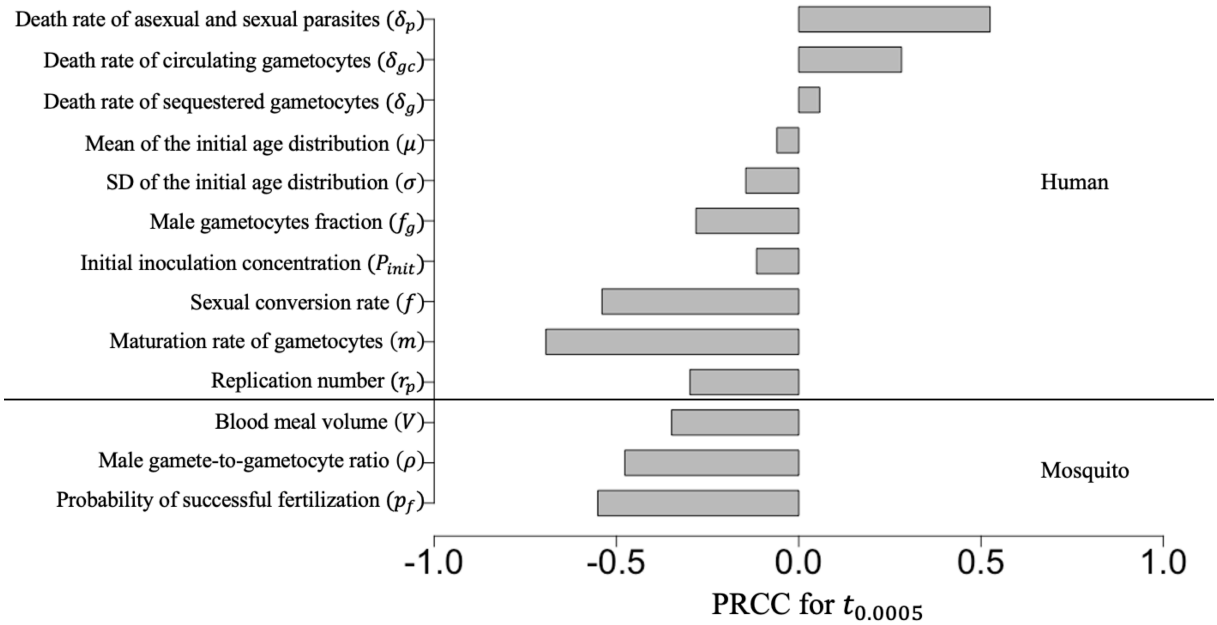

PRCC results between parameters and $t_{0.001}$ (top) and $t_{0.0005}$ (bottom) for low transmission settings.

S7 Fig.

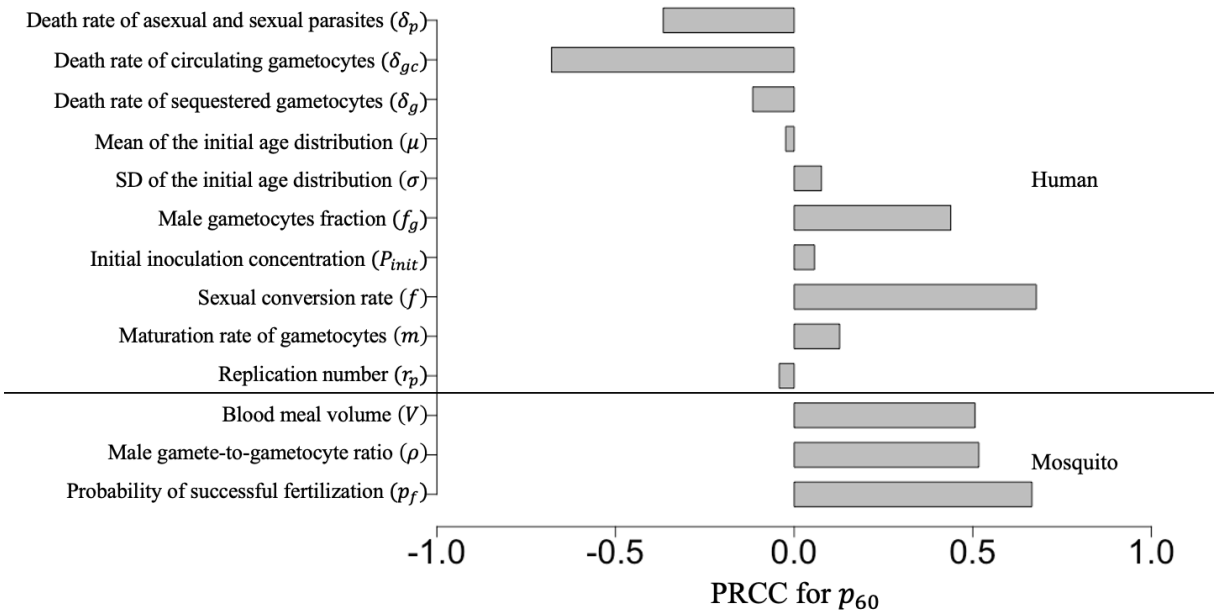

PRCC results between parameters and p_{60} for low transmission settings.

S8 Fig.

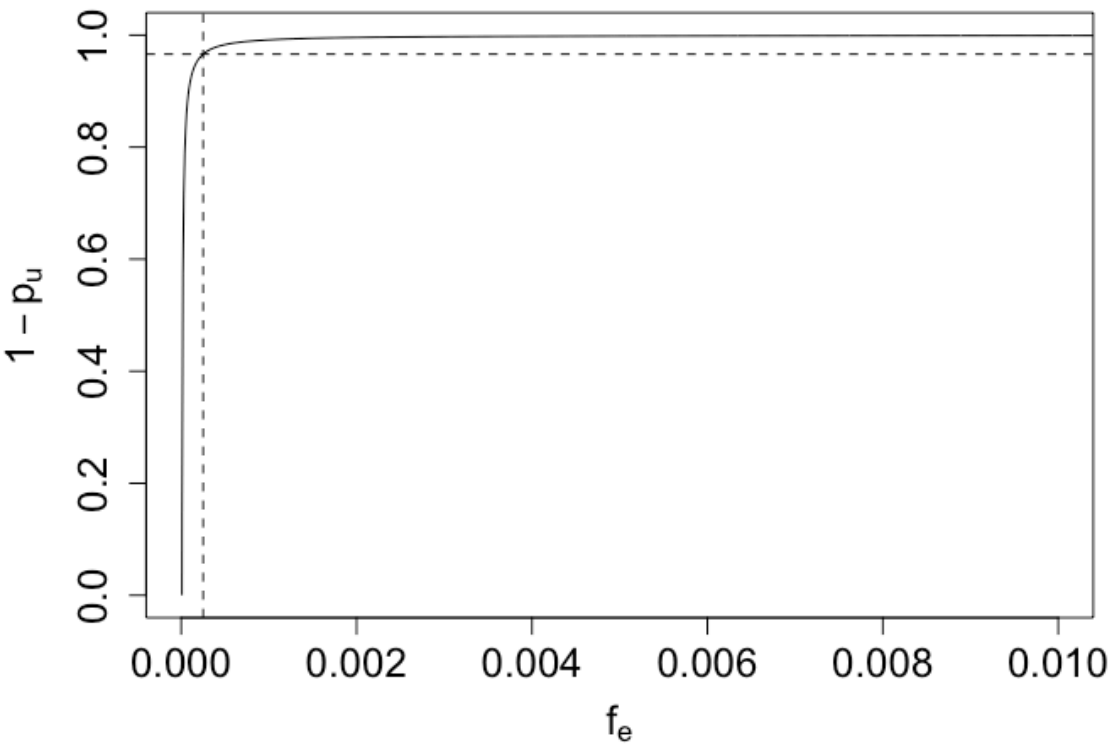

Relationship between f_e and $1 - p_u$. The plot illustrates how changes in f_e influence the variance of the binomial distributions determining the number of male and female gametocytes

taken by a mosquito during a blood meal, which is given by $\mathrm{Var}(G_{\{M,F\}}) = G_{\{M,F\}} f_e p_u (1-p_u) = G_{\{M,F\}} \frac{V}{V_H}(1 - \frac{V}{V_H f_e}) \propto (1 - p_u)$. The dashed lines represent the benchmark value of f_e and corresponding $1 - p_u$.

References

[1] The World Health Organization. World malaria report 2025: addressing the threat of antimalarial drug resistance. Technical report, Geneva: World Health Organization, 2025.

[2] G. A. Josling and M Llinás. Sexual development in plasmodium parasites: knowing when it's time to commit. *Nature Reviews Microbiology*, 13(9):573–587, 2015.

[3] Petra Schneider, Louis Clément Gouagna, Sabah Ahmed Omar, Silas Otieno, J. Teun Bousema, Robert W. Sauerwein, and Marga van de Vegte-Bolmer. Submicroscopic plasmodium falciparum gametocyte densities frequently result in mosquito infection. *The American journal of tropical medicine and hygiene*, 76 3:470–4, 2007.

[4] André Lin Ouédraogo, Teun Bousema, Petra Schneider, Sake J. de Vlas, Edith Ilboudo-Sanogo, Nadine Cuzin-Ouattara, Issa Nebie', Will F. G. Roeffen, Jan Peter Verhave, Adrian J F Luty, and Robert W. Sauerwein. Substantial contribution of submicroscopical plasmodium falciparum gametocyte carriage to the infectious reservoir in an area of seasonal transmission. *PLoS ONE*, 4, 2009.

[5] Bronner P. Gonçalves, Melissa C. Kapulu, Patrick Sawa, Wamdaogo Moussa Guelbéogo, Alfred B. Tiono, Lynn Grignard, Will Stone, Joel Hellewell, Kjerstin Lanke, Guido J. H. Bastiaens, John Bradley, Issa Nebie', Joyce Mwongeli Ngoi, Robin M Oriango, Dora Mkabili, Maureen Nyaurah, Janet Midega, Dyann F. Wirth, Kevin Marsh, Thomas S. Churcher, Philip Bejon, Sodiomon B. Sirima, Christopher J. Drakeley, and Teun Bousema. Examining the human infectious reservoir for plasmodium falciparum malaria in areas of differing transmission intensity. *Nature Communications*, 8, 2017.

[6] Luke Anthony Baton and Lisa C. Ranford-Cartwright. Spreading the seeds of million-murdering death: metamorphoses of malaria in the mosquito. *Trends in parasitology*, 21 12:573–80, 2005.

[7] Robert E Sinden. The cell biology of sexual development in plasmodium. *Parasitology*, 86:7 – 28, 1983.

[8] Noriko Okamoto, Timothy P. Spurck, Christopher Dean Goodman, and Geoffrey Ian McFadden. Apicoplast and mitochondrion in gametocytogenesis of plasmodium falciparum. *Eukaryotic Cell*, 8:128 – 132, 2008.

[9] Robert E Sinden, Arthur M. Talman, Sara Rute Marques, Mark N. Wass, and Michael J. E. Sternberg. The flagellum in malarial parasites. *Current opinion in microbiology*, 13 4:491–500, 2010.

[10] Thomas S. Churcher, Teun Bousema, Martin Walker, Christopher J. Drakeley, Petra Schneider, André Lin Ouédraogo, and María-Gloria Basáñez. Predicting mosquito infection from plasmodium falciparum gametocyte density and estimating the reservoir of infection. *eLife*, 2, 2013.

[11] Katharine A. Collins, Claire Y. T. Wang, Matthew Adams, Hayley Mitchell, Melanie Rampton, Suzanne Elliott, Isaie J. Reuling, Teun Bousema, Robert W. Sauerwein, Stephan Chalon, Jörg J. Möhrle, and James S. McCarthy. A controlled human malaria infection model enabling evaluation of transmission-blocking interventions. *The Journal of Clinical Investigation*, 128:1551 – 1562, 2018.

[12] John Bradley, Will Stone, Dari F Da, Isabelle Morlais, Alassane Dicko, Anna Cohuet, Wamdaogo Moussa Guelbéogo, Almahamoudou Mahamar, Sandrine Eveline Nsango, Harouna M Soumare, Halimatou Diawara, Kjerstin H. W. Lanke, Wouter Graumans, Rianne Siebelink-Stoter, Marga G. van de Vegte-Bolmer, Ingrid T Chen, Alfred B. Tiono, Bronner P Gonçalves, Roland D. Gosling, Robert W. Sauerwein, Christopher J. Drakeley, Thomas S. Churcher, and Teun Bousema. Predicting the likelihood and intensity of mosquito infection from sex specific plasmodium falciparum gametocyte density. *eLife*, 7, 2018.

[13] Teun Bousema, Lucy C. Okell, Ingrid Felger, and Christopher J. Drakeley. Asymptomatic malaria infections: detectability, transmissibility and public health relevance. *Nature Reviews Microbiology*, 12:833–840, 2014.

[14] Harouna M Soumare, Sara Lynn Blanken, Abdullahi Ahmad, Michael Ooko, Pa Modou Gaye, Lamin Jadama, Muhammed M. Camara, Ebrima A. Jawara, Kjerstin Lanke,

Amie Kolleh Njie, Michael Mendy, Blessed Etoketim, Lamin Camara, Mamadou O Ndiath, Bakary Conteh, Nuredin Muhammed, Seyi Soremekun, Abdoullah Nyassi, Annette Erhart, Chris J. Drakeley, Teun Bousema, Umberto d'Alessandro, and Marta Moreno. Asymptomatic school children and adults are important for the human infectious reservoir for plasmodium falciparum malaria in an area of low endemicity in the gambia. *The Journal of Infection*, 91, 2025.

[15] Moshe B Hoshen, Reinhart Heinrich, Wilfred Donald Stein, and Hagai Ginsburg. Mathematical modelling of the within-host dynamics of plasmodium falciparum. *Parasitology*, 121:227 – 235, 2000.

[16] Sompob Saralamba, Wirichada Pan-ngum, Richard James Maude, Sue J Lee, Joel Tarning, Niklas Lindegårdh, Kesinee Chotivanich, François H. Nosten, Nicholas P. J. Day, Duong Socheat, Nicholas J. White, Arjen M. Dondorp, and Lisa Jane White. Intrahost modeling of artemisinin resistance in plasmodium falciparum. *Proceedings of the National Academy of Sciences*, 108:397 – 402, 2010.

[17] Sophie G. Zaloumis, Andrew Jonathan Humberstone, Susan A. Charman, Ric N. Price, Joerg J. Moehrle, Javier Gamo-Benito, James M. McCaw, Kris M. Jamsen, Katherine Smith, and Julie Anne Simpson. Assessing the utility of an anti-malarial pharmacokinetic-pharmacodynamic model for aiding drug clinical development. *Malaria Journal*, 11:303 – 303, 2012.

[18] Martin Eichner, Hans H. Diebner, Louis Molineaux, William E. Collins, Geoffrey M. Jeffery, and Klaus Dietz. Genesis, sequestration and survival of plasmodium falciparum gametocytes: parameter estimates from fitting a model to malariatherapy data. *Transactions of the Royal Society of Tropical Medicine and Hygiene*, 95 5:497–501, 2001.

[19] P. Cao, K. A. Collins, S. Zaloumis, T. Wattanakul, and J. M. Mccaw. Modeling the dynamics of plasmodium falciparum gametocytes in humans during malaria infection. *eLife*, 8, 2019.

[20] Xiao Sun, James M. McCaw, and Pengxing Cao. Stochastic modeling of within-host dynamics of plasmodium falciparum. *Mathematics*, 10(21), 2022.

[21] Miranda Ijang Teboh-Ewungkem and Thomas Yuster. A within-vector mathematical model of plasmodium falciparum and implications of incomplete fertilization on optimal gameto-

cyte sex ratio. *Journal of theoretical biology*, 264 2:273–86, 2010.

[22] Lauren M. Childs and Olivia F. Prosper. Simulating within-vector generation of the malaria parasite diversity. *PLoS ONE*, 12, 2017.

[23] Miranda Ijang Teboh-Ewungkem, Woldegebriel Assefa Woldegerima, and Gideon A. Ngwa. Mathematical assessment of the impact of human-antibodies on sporogony during the within-mosquito dynamics of plasmodium falciparum parasites. *Journal of theoretical biology*, page 110562, 2020.

[24] Lauren M. Childs and Olivia F. Prosper. The impact of within-vector parasite development on the extrinsic incubation period. *Royal Society Open Science*, 7, 2020.

[25] Isaac J. Stopard, Thomas S. Churcher, and Ben Lambert. Estimating the extrinsic incubation period of malaria using a mechanistic model of sporogony. *PLoS Computational Biology*, 2021.

[26] Philip A Eckhoff and Edward A Wenger. The emod individual-based model. *Spatial Agent-Based Simulation Modeling in Public Health: Design, Implementation, and Applications for Malaria Epidemiology*, pages 185–208, 2016.

[27] Tobias Thüring, Diggory Hardy, Aurélien Cavelan, ThomasASmith, Dominic Jodoin, Making GitHub Delicious., Melissa Penny, nakul7, obriet, pemberto, and rogoersTPH. Swisstph/openmalaria: Release schema-46.0, January 2024.

[28] Christina Salgado, George Ayodo, Michael D. Macklin, Meetha P. Gould, Srinivas Nallandhighal, Eliud O. Odhiambo, Andrew Ambogo Obala, Wendy Prudhomme O'Meara, Chandy C. John, and Tuan M. Tran. The prevalence and density of asymptomatic plasmodium falciparum infections among children and adults in three communities of western kenya. *Malaria Journal*, 20, 2021.

[29] André Barembaye Sagna, Yilekal Gebre, Claudia A. Vera-Arias, Dipomin François Traoré, Bertin N'cho Tchekoi, Serge Brice Assi, Amnan Alphonsine Koffi, Christophe Rogier, Franck Remoue, and Cristian Koepfli. High prevalence of asymptomatic and subpatent plasmodium falciparum infections but no histidine-rich protein 2 gene deletion in bouaké, côte d'ivoire. *Scientific Reports*, 14, 2024.

[30] Kim A. Lindblade, Laura C. Steinhardt, Aaron M. Samuels, S. Patrick Kachur, and Laurence Slutsker. The silent threat: asymptomatic parasitemia and malaria transmission. *Expert Review of Anti-infective Therapy*, 11:623 – 639, 2013.

[31] Fitsum Girma Tadesse, Lotus Leonie van den Hoogen, Kjerstin Lanke, Jodie A. Schildkraut, Kevin K.A. Tetteh, Abraham Aseffa, Hassen Mamo, Robert W. Sauerwein, Ingrid Felger, Christopher J. Drakeley, Endalamaw Gadissa, and Teun Bousema. The shape of the iceberg: quantification of submicroscopic plasmodium falciparum and plasmodium vivax parasitaemia and gametocytaemia in five low endemic settings in ethiopia. *Malaria Journal*, 16, 2017.

[32] Hannah C. Slater, Amanda Ross, Ingrid Felger, Natalie E Hofmann, Leanne J. Robinson, Jackie Cook, Bronner P. Gonçalves, Anders Björkman, André Lin Ouédraogo, Ulrika Morris, Mwinyi I. Msellem, Cristian Koepfli, Ivo Mueller, Fitsum Girma Tadesse, Endalamaw Gadisa, Smita Das, Gonzalo J Domingo, Melissa C. Kapulu, Janet Midega, Seth Owusu-Agyei, Cécile Nabet, Renaud Piarroux, Ogobara K. Doumbo, Safiatou Niaré Doumbo, Kwadwo Ansah Koram, Naomi W Lucchi, Venkatachalam Udhayakumar, Jacklin F. Mosha, Alfred B. Tiono, Daniel Chandramohan, Roly Gosling, Felista Mwingira, Robert W. Sauerwein, Richard Paul, Eleanor M. Riley, Nicholas J. White, François H. Nosten, Mallika Imwong, Teun Bousema, Christopher J. Drakeley, and Lucy C. Okell. The temporal dynamics and infectiousness of subpatent plasmodium falciparum infections in relation to parasite density. *Nature Communications*, 10, 2019.

[33] Katharine A. Collins, Sukai Ceesay, Sainabou Drammeh, Fatou Jaiteh, Marc-Antoine Guery, Kjerstin Lanke, Lynn Grignard, Will Stone, David J. Conway, Umberto D'Alessandro, Teun Bousema, and Antoine Claessens. A cohort study on the duration of plasmodium falciparum infections during the dry season in the gambia. *The Journal of Infectious Diseases*, 226:128 – 137, 2021.

[34] Dianna E. B. Hergott, Tonny Jimmy Owalla, Weston J Staubus, Annette M. Seilie, Chris Chavtur, Jennifer E Balkus, Bernadette Apio, Jimmy Lema, Barbara Cemeri, Andrew Akileng, Ming Chang, Thomas G. Egwang, and Sean C. Murphy. Assessing the daily natural history of asymptomatic plasmodium infections in adults and older children in katakwi, uganda: a longitudinal cohort study. *The Lancet. Microbe*, 5:e72 – e80, 2023.

[35] Sandip Mandal, Ram Rup Sarkar, and Somdatta Sinha. Mathematical models of malaria - a review. *Malaria Journal*, 10:202 – 202, 2011.

[36] Simeone Marino, Ian B. Hogue, Christian J Ray, and Denise E. Kirschner. A methodology for performing global uncertainty and sensitivity analysis in systems biology. *Journal of theoretical biology*, 254 1:178–96, 2008.

[37] Teun Bousema and Christopher J. Drakeley. Epidemiology and infectivity of plasmodium falciparum and plasmodium vivax gametocytes in relation to malaria control and elimination. *Clinical Microbiology Reviews*, 24:377 – 410, 2011.

[38] Ernest Mazigo, Hojong Jun, Wang-Jong Lee, Johnsy Mary Louis, Fadhila Fitriana, Jadidan Hada Syahada, Fauzi Muh, Feng Lu, Md Atique Ahmed, Seok Ho Cha, Wanjoo Chun, Won Sun Park, Se Jin Lee, Sunghun Na, Joon-Hee Han, Nyalali Kija, Smart Geodfrey, Eun-Taek Han, Jim Todd, Alphaxard Manjurano, Winifrida B Kidima, and Jin-Hee Han. Prevalence of asymptomatic malaria in high- and low-transmission areas of tanzania: The role of asymptomatic carriers in malaria persistence and the need for targeted surveillance and control efforts. *Parasites, Hosts and Diseases*, 63:57 – 65, 2025.

[39] Emily R. Ebel, Frans A. Kuypers, Carrie Lin, Dmitri A. Petrov, and Elizabeth S. Egan. Common host variation drives malaria parasite fitness in healthy human red cells. *eLife*, 10, 2020.

[40] Suprita Singh, Joana M. Santos, Lindsey M. Orchard, Naomi Yamada, Riëtte van Biljon, Heather J. Painter, Shaun Mahony, and Manuel Llinás. The pfap2-g2 transcription factor is a critical regulator of gametocyte maturation. *bioRxiv*, 2020.

[41] Alexander D. Douglas, Laura Andrews, Simon J. Draper, Kalifa A. Bojang, Paul Milligan, Sarah C. Gilbert, Egeruan Babatunde Imoukhuede, and Adrian V. S. Hill. Substantially reduced pre-patent parasite multiplication rates are associated with naturally acquired immunity to plasmodium falciparum. *The Journal of infectious diseases*, 203 9:1337–40, 2011.

[42] Louis Molineaux, Hans H. Diebner, Martin Eichner, William E. Collins, Geoffrey M. Jeffery, and Klaus Dietz. Plasmodium falciparum parasitaemia described by a new mathematical model. *Parasitology*, 122:379 – 391, 2001.

[43] Lauren M. Childs and Caroline O. Buckee. Dissecting the determinants of malaria chronicity: why within-host models struggle to reproduce infection dynamics. *Journal of the Royal Society Interface*, 12, 2015.

[44] Lei Zhu, Jaishree Tripathi, Frances Rocamora, Olivo Miotto, Rob W. van der Pluijm, Till S. Voss, Sachel Mok, Dominic P. Kwiatkowski, François H. Nosten, Nicholas P. J. Day, Nicholas J. White, Arjen M. Dondorp, Zbynek Bozdech, Aung Pyae Elizabeth A. Frank Khin Kyaw Myo M Abul Mayfo Phyo Ashley Smithuis Lin Tun Faiz Mayxay Dhorda Th, Aung Pyae Phyo, Elizabeth A. Ashley, Frank M. Smithuis, Khin Lin, Kyaw Myo Tun, M. Abul Faiz, Mayfong Mayxay, Mehul Dhorda, Nguyen T Thuy-Nhien, Paul N. Newton, Sasithon Pukrittayakamee, Tin Maung Hlaing, Tran Tinh Hien, and Ye Htut. The origins of malaria artemisinin resistance defined by a genetic and transcriptomic background. *Nature Communications*, 9, 2018.

[45] Harvie P. Portugaliza, Shinya Miyazaki, Fiona J. A. Geurten, Christopher Pell, Anna Rosanas-Urgell, Chris J. Janse, and Alfred Cortés. Artemisinin exposure at the ring or trophozoite stage impacts plasmodium falciparum sexual conversion differently. *eLife*, 9, 2020.

[46] Harvie P. Portugaliza, Hamatandi Magloire Natama, Pieter Guetens, Eduard Rovira-Vallbona, Athanase Mwinessobaonfou Somé, Aida Millogo, Delwendé Florence Ouedraogo, Innocent Valéa, Hermann Sorgho, Halidou Tinto, Nguyen Van Hong, António Sitoe, Rosauro Varo, Quique Bassat, Alfred Cortés, and Anna Rosanas-Urgell. Plasmodium falciparum sexual conversion rates can be affected by artemisinin-based treatment in naturally infected malaria patients. *eBioMedicine*, 83, 2022.

[47] Chiara Andolina, Jordache Ramjith, John Rek, Kjerstin Lanke, Joseph Okoth, Lynn Grignard, Emmanuel Arinaitwe, Jessica Briggs, Jeffrey A. Bailey, Ozkan Aydemir, Moses R. Kamya, Bryan Greenhouse, Grant Dorsey, Sarah G. Staedke, Christopher J. Drakeley, Marianne Jonker, and Teun Bousema. Plasmodium falciparum gametocyte carriage in longitudinally monitored incident infections is associated with duration of infection and human host factors. *Scientific Reports*, 13, 2023.

[48] Nicholas J. White. Primaquine to prevent transmission of falciparum malaria. *The Lancet. Infectious diseases*, 13 2:175–81, 2013.

[49] Palang Chotsiri, Almahamoudou Mahamar, Richard M Hoglund, Fanta Koita, Koualy Sanogo, Halimatou Diawara, Alassane Dicko, Julie A. Simpson, Teun Bousema, Nicholas J. White, Joelle M Brown, Roly Gosling, Ingrid T Chen, and Joel Tarning. Mechanistic modeling of primaquine pharmacokinetics, gametocytocidal activity, and mosquito infectivity. *Clinical Pharmacology and Therapeutics*, 111:676 – 685, 2021.

[50] Mayumi Tachibana, Eizo Takashima, Motomi Torii, Yimin Wu, Jetsumon Sattabongkot, and Takafumi Tsuboi. Advances in transmission-blocking vaccines against plasmodium falciparum and plasmodium vivax. *Expert review of vaccines*, 2025.

[51] Andargie Abate, Soriya Kedir, Mitiku Bose, Jifar Hassen, Laurent Dembélé, and Lemu Golassa. Infectivity of symptomatic patients and their contribution for infectiousness of mosquitoes following a membrane feeding assay in ethiopia. *Microbiology Spectrum*, 10, 2022.

[52] C. C. Murdock, Eleanore D. Sternberg, and M. Benson Thomas. Malaria transmission potential could be reduced with current and future climate change. *Scientific Reports*, 6, 2016.

[53] Lillian L M Shapiro, Courtney C. Murdock, Gregory R. Jacobs, Rachel J. Thomas, and Matthew B. Thomas. Larval food quantity affects the capacity of adult mosquitoes to transmit human malaria. *Proceedings of the Royal Society B: Biological Sciences*, 283, 2016.

[54] Sandra Bennink, Meike J. Kiesow, and Gabriele Pradel. The development of malaria parasites in the mosquito midgut. *Cellular Microbiology*, 18:905 – 918, 2016.

[55] April M. Clayton, Yuemei Dong, and George Dimopoulos. The anopheles innate immune system in the defense against malaria infection. *Journal of Innate Immunity*, 6:169 – 181, 2013.

[56] Emma Pietsch, Korbinian Niedermüller, Mia Andrews, Britta S. Meyer, Tobias L Lenz, Danny W. Wilson, Tim W. Gilberger, and Paul-Christian Burda. Disruption of a plasmodium falciparum patatin-like phospholipase delays male gametocyte exflagellation. *Molecular Microbiology*, 121:529 – 542, 2023.

[57] Thomas S. Churcher, Robert E Sinden, Nick J. Edwards, Ian D. Poulton, Tommy Rampling, Patrick M. Brock, Jamie T. Griffin, Leanna M. Upton, Sara E Zakutansky, Katarzyna A. Sala, Fiona Angrisano, Adrian V. S. Hill, and Andrew M. Blagborough. Probability of transmission of malaria from mosquito to human is regulated by mosquito parasite density in naïve and vaccinated hosts. *PLoS Pathogens*, 13, 2017.

[58] Wouter Graumans, Roel Heutink, Geert-Jan van Gemert, Marga G. van de Vegte-Bolmer, Teun Bousema, and Katharine A. Collins. A mosquito feeding assay to examine plasmodium transmission to mosquitoes using small blood volumes in 3d printed nano-feeders. *Parasites & Vectors*, 13, 2020.

[59] Scott Anthony Sisson, Y. Fan, and Mark M. Tanaka. Sequential monte carlo without likelihoods. *Proceedings of the National Academy of Sciences*, 104:1760 – 1765, 2007.

[60] Pablo Suárez-Cortés, Giulia Costa, Manuela Andres, Daniel Eyermann, Cornelia Kreschel, Liane Spohr, Christian Goosmann, Volker Brinkmann, and Elena A. Levashina. Generation of a plasmodium falciparum reporter line for studies of parasite biology throughout the life cycle. *bioRxiv*, 2023.

[61] Yannik Schälte and Jan Hasenauer. Informative and adaptive distances and summary statistics in sequential approximate bayesian computation. *PLOS ONE*, 18, 2022.

[62] Maxime Lenormand, Franck Jabot, and Guillaume Deffuant. Adaptive approximate bayesian computation for complex models. *Computational Statistics*, 28:2777–2796, 2013.

[63] Daniel T. Gillespie. Approximate accelerated stochastic simulation of chemically reacting systems. *J. Chem. Phys.*, 115:1716–1733, 2001.

[64] Zbynek Bozdech, Manuel Llinás, Brian Pulliam, Edith D. Wong, Jingchun Zhu, and Joseph L. Derisi. The transcriptome of the intraerythrocytic developmental cycle of plasmodium falciparum. *PLoS Biology*, 1, 2003.

[65] Fitsum Girma Tadesse, Lisette Meerstein-Kessel, Bronner P. Gonçalves, Christopher J. Drakeley, Lisa C. Ranford-Cartwright, and Teun Bousema. Gametocyte sex ratio: The key to understanding plasmodium falciparum transmission? *Trends in Parasitology*, 35:226 – 238, 2019.

[66] Emma J Dawes, Thomas S. Churcher, Shijie Zhuang, Robert E Sinden, and María-Gloria Basáñez. Anopheles mortality is both age- and plasmodium-density dependent: implications for malaria transmission. *Malaria Journal*, 8:228 – 228, 2009.

[67] Sarah Filippi, Chris P. Barnes, Julien Cornebise, and Michael P.H. Stumpf. On optimality of kernels for approximate bayesian computation using sequential monte carlo. *Statistical Applications in Genetics and Molecular Biology*, 12(1):87–107, 2013.